Structure and properties of small-scale magnetic fields
Part I

Luis Bellot Rubio
Instituto de Astrofísica de Andalucía (IAA-CSIC)

ISSS "The many spatio-temporal scales of solar magnetism", L'Aquila , 11-15 April 2022

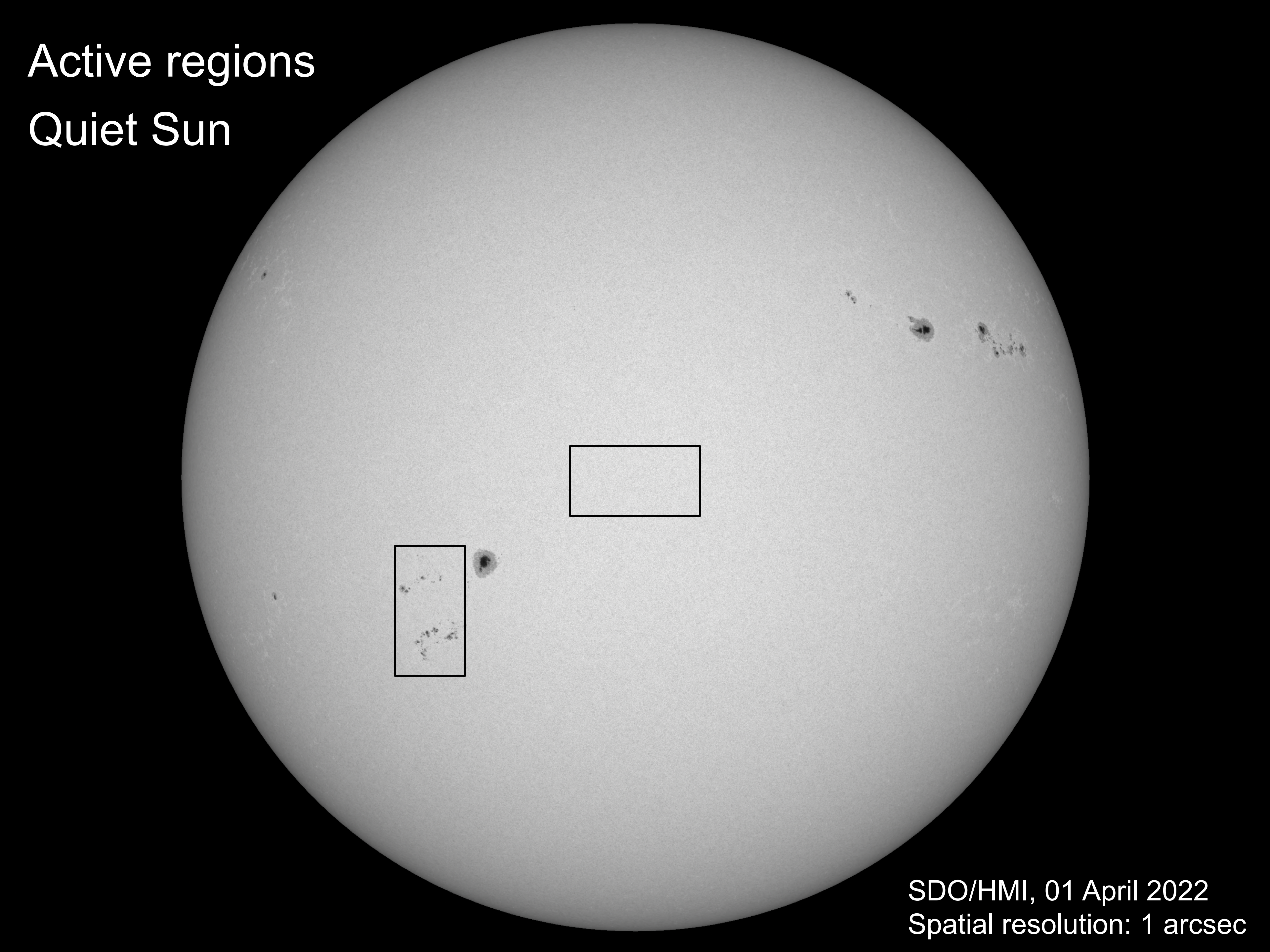
Active regions
Quiet Sun
SDO/HMI, 01 April 2022
Spatial resolution: 1 arcsec

The quiet Sun

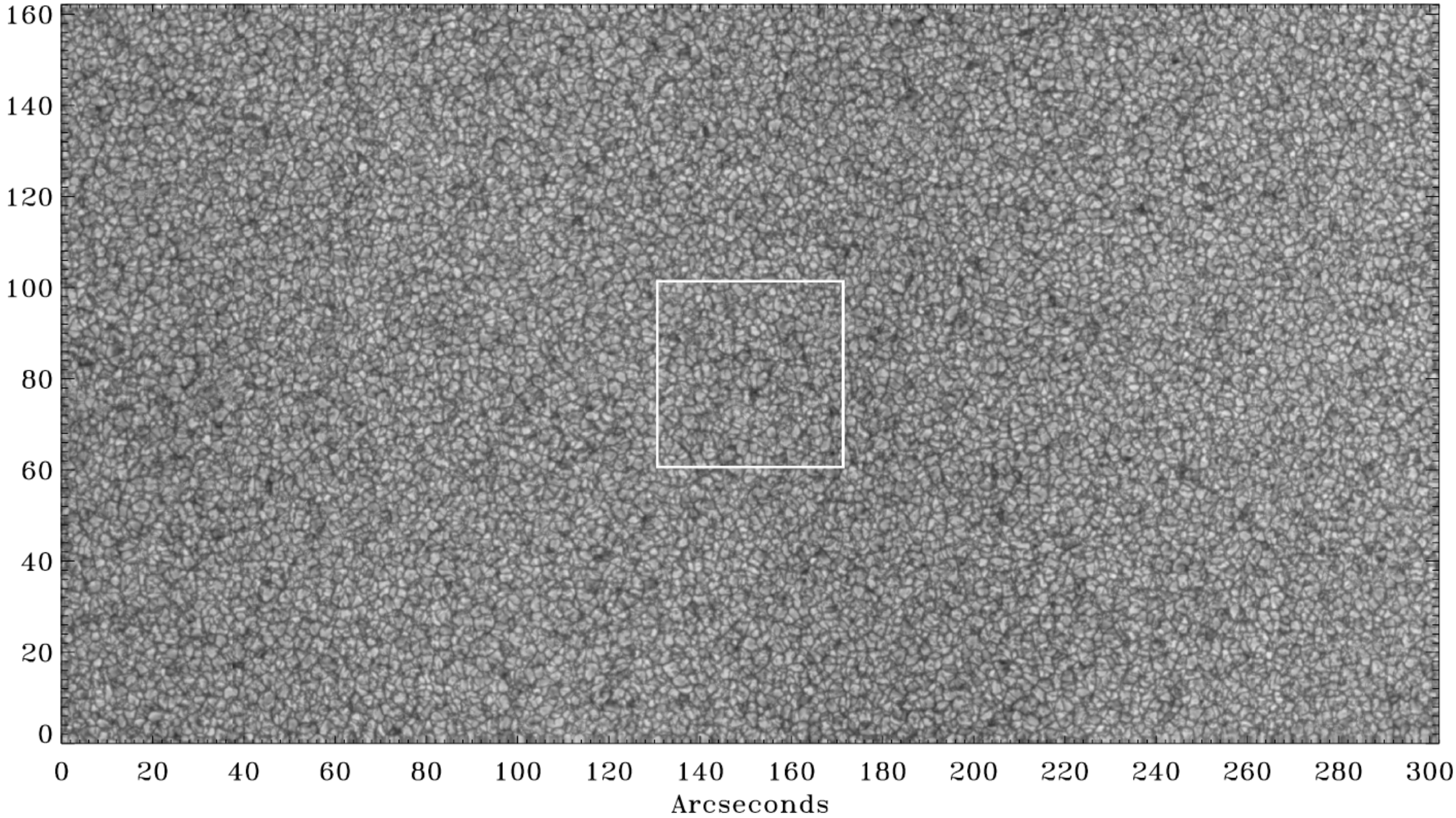

Lites et al., 2008, ApJ, 672, 1237

Hinode/SP normal map, Fe I 630 nm
Integration time: 4.8 s

0.5m telescope, seeing-free conditions
Spatial resolution: 0.3 arcsec

The quiet Sun

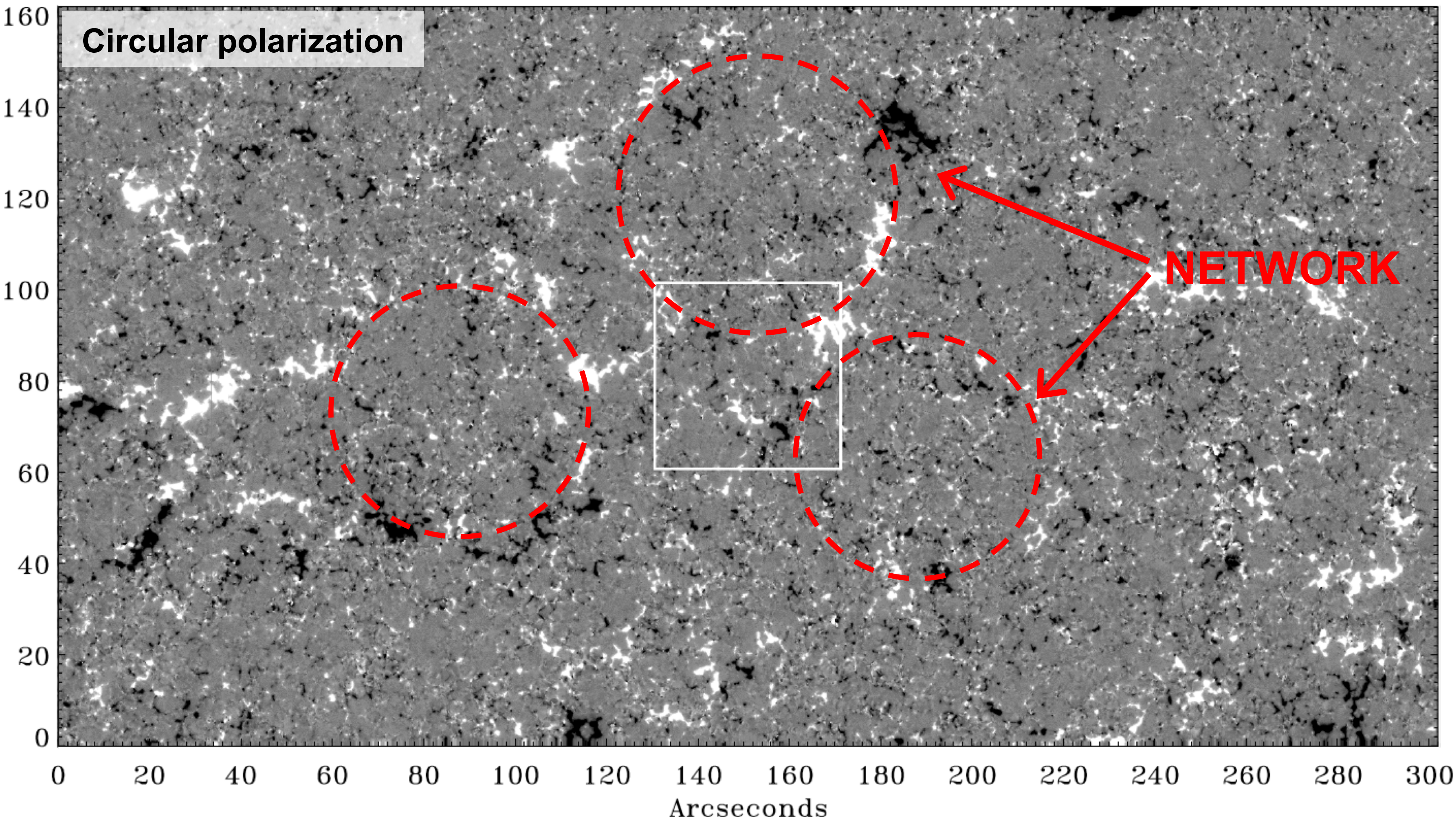

Lites et al., 2008, ApJ, 672, 1237

Hinode/SP normal map, Fe I 630 nm
Noise level: 1.1 x 10^{-3} I_c

- Network delineates supergranular cells
- Strong polarization signals in network
- Weak signals in cell interior

Active regions

Network

Internetwork

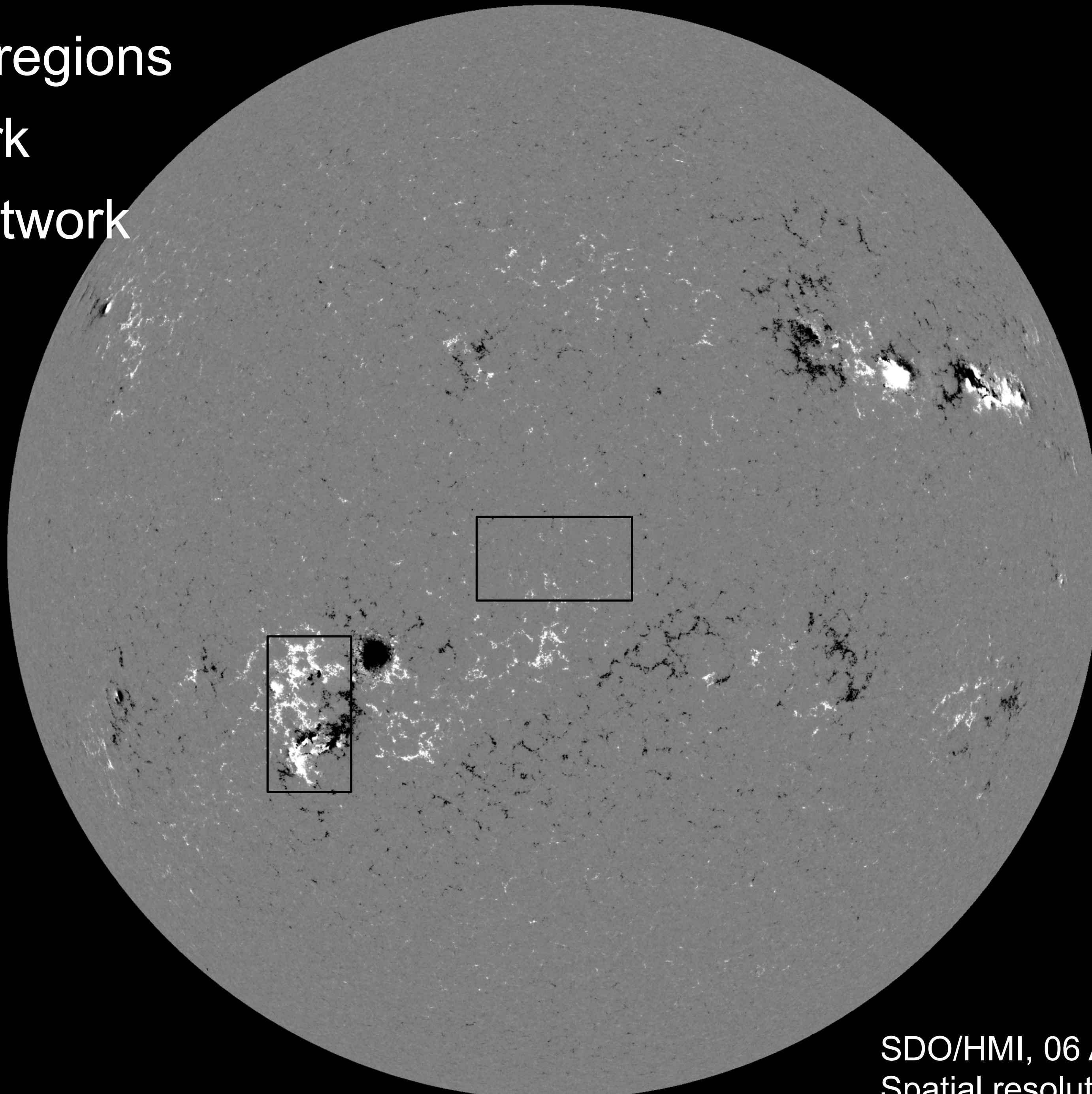

SDO/HMI, 06 April 2022

Spatial resolution: 1 arcsec

Outline

- The quiet Sun
- Quiet Sun magnetic fields
  - Properties and required observations
  - Quiet Sun flux budget
- Magnetic network
  - Network magnetic fields and supergranulation
  - Properties of kG flux tubes
  - Formation of kG fields
  - Origin of network fields
- Quiet Sun internetwork
  - Magnetic properties at high spatial resolution
  - Magnetic topology
  - Flux appearance processes: unipolar vs bipolar appearance
- Open questions
  - Origin of internework fields
  - Magnetic coupling by quiet Sun
  - Role of QS fields in heating the upper atmosphere

Quiet Sun magnetic fields

- Create large patterns on solar surface (network/internetwork)
- Everywhere on the solar surface, all the time
- Enormous amount of magnetic flux

- Organized on very small spatial scales (of order 0.1”)
- Weak fields for the most part
- Highly dynamic
  - Short lifetimes
  - Interact with convective flows and other magnetic fields
  - Contribute to atmospheric heating and dynamics
  - Connect the different layers of the solar atmosphere

- Full Stokes spectropolarimetry (Zeeman and Hanle effects)
- High spatial resolution, sensitivity and temporal resolution needed

Zeeman spectropolarimetry at high resolution

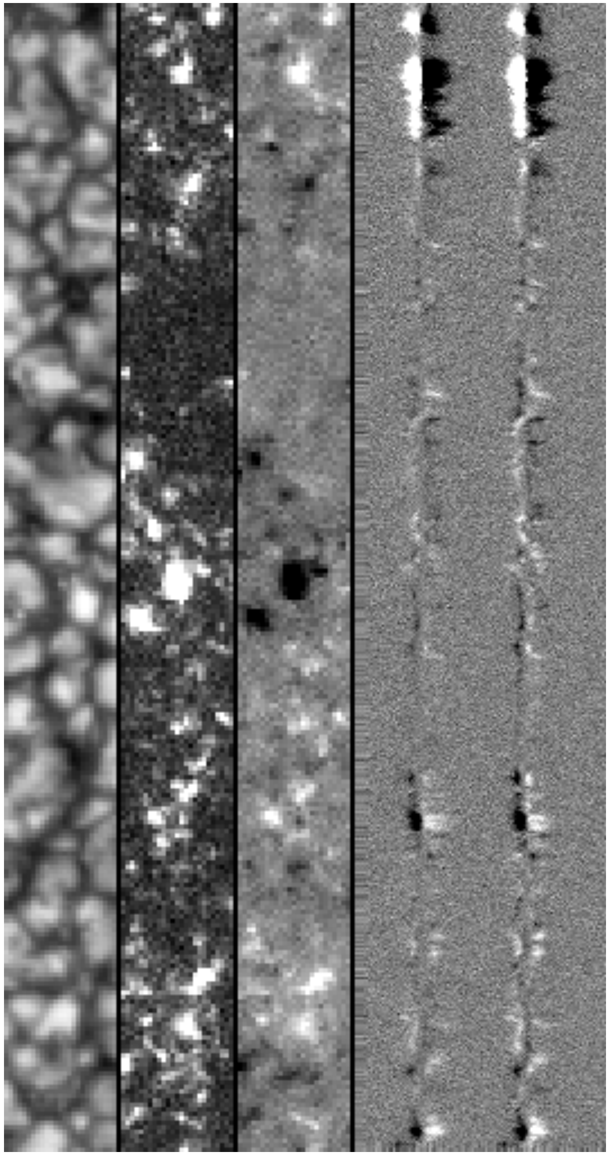

Quiet Sun magnetism

2007-02-11 11:07:08.0 to 2007-02-10 15:39:52.0
Science Goal: Quiet Sun magnetism
Program: SP normal map
Target: disk center
Pointing: xcen=0 ycen=-80

Exposure time:	4.8 s/slit
Pixel size:	0.16″
FOV:	4″ x 164″
Cadence:	2 min
Noise level:	$1.1 \times 10^{-3}\ I_c$

The importance of spatial resolution

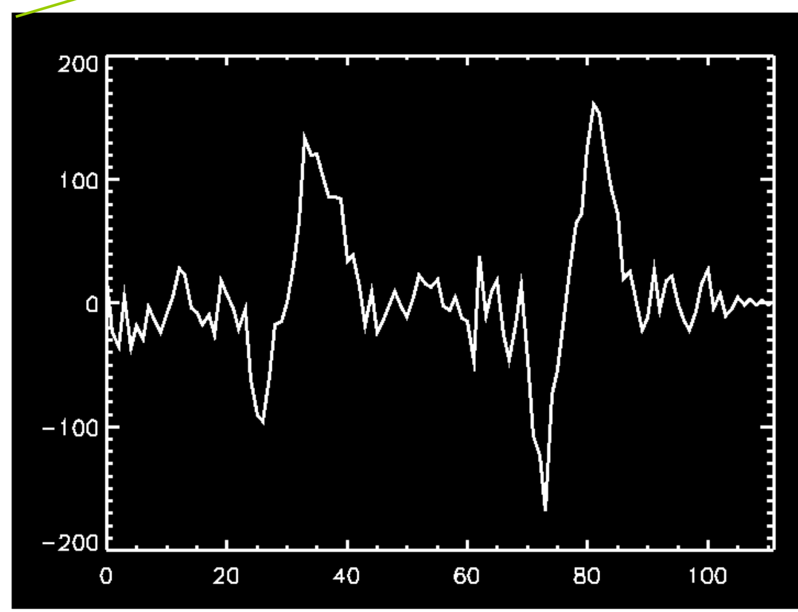

Hinode/SP, 25 Sep 2007, 15:00 UT
Exposure time: 1.6 s/slit
Spatial resolution: 0.32"

The importance of spatial resolution

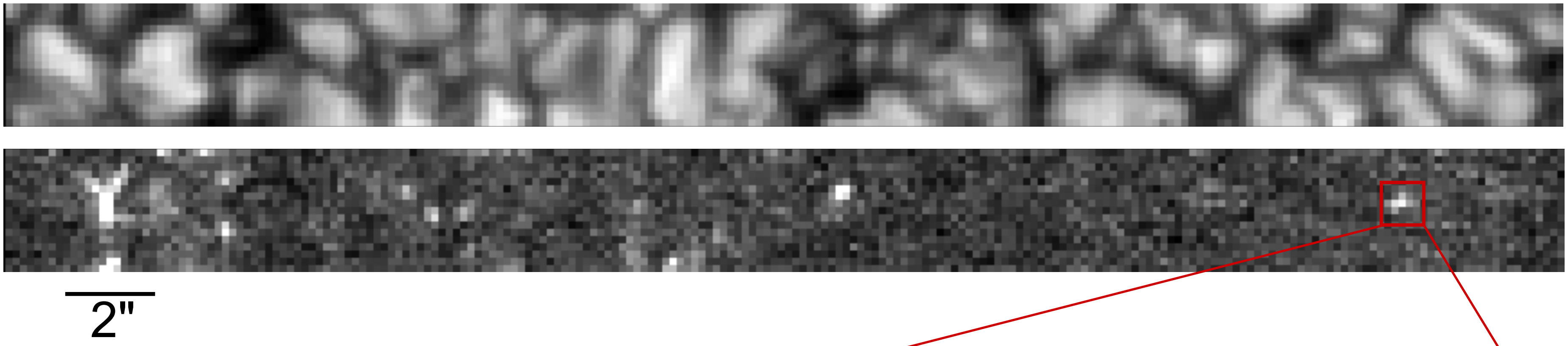

Hinode/SP, 25 Sep 2007, 15:00 UT
Exposure time: 1.6 s/slit
Spatial resolution: 0.32"

Spatial resolution: 0.8"
Stokes V signal is 5 times smaller!

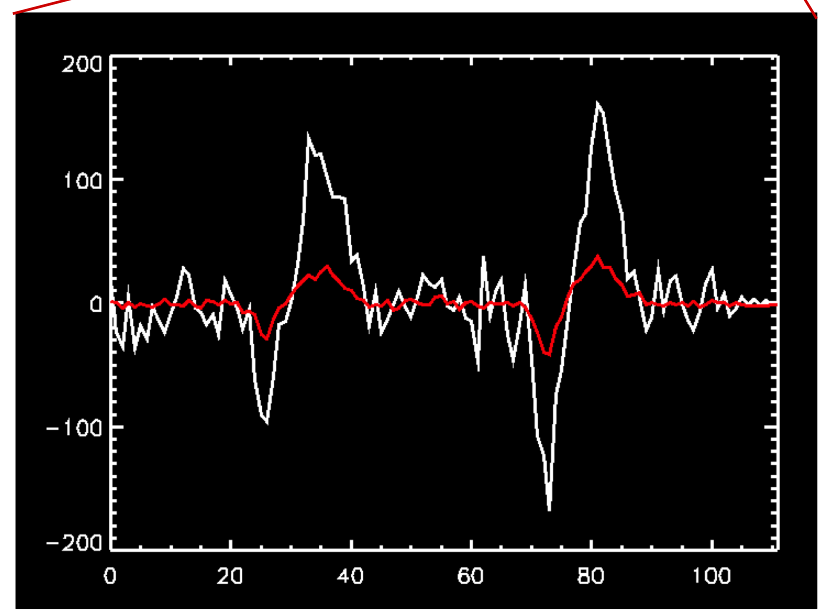

The importance of polarimetric sensitivity

Quiet Sun fields are weak and produce very small polarization signals

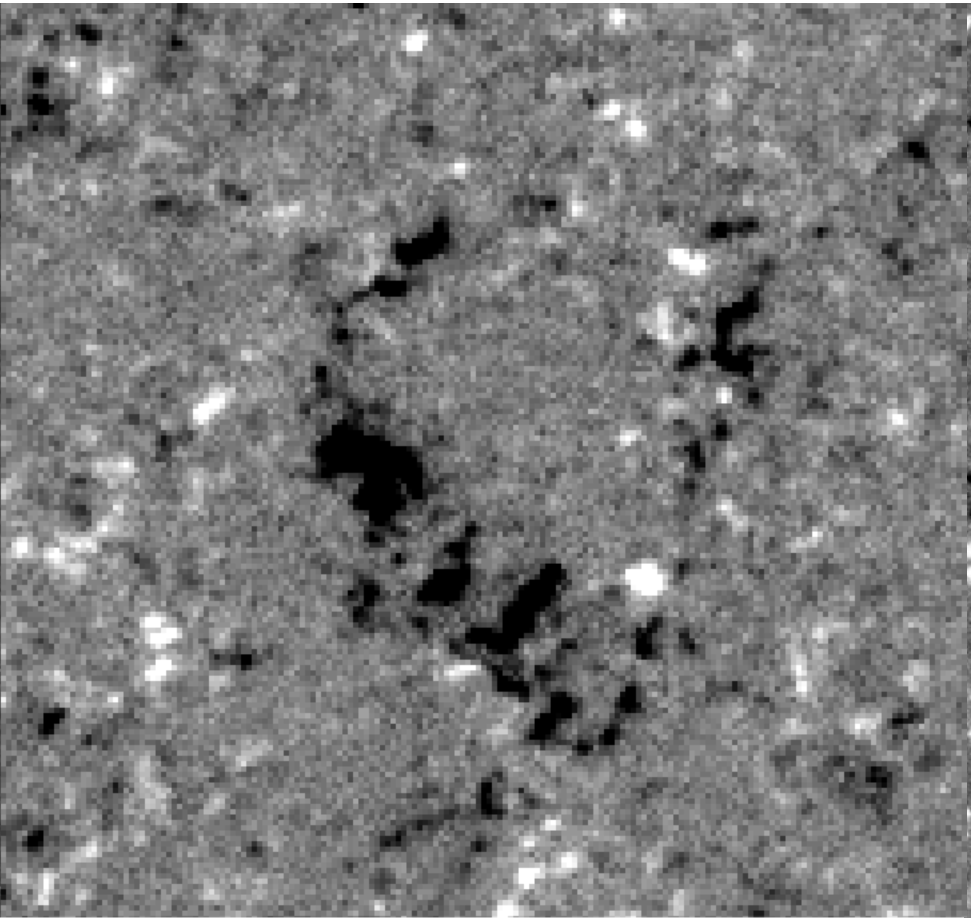

SDO/HMI 720s Stokes V measurements

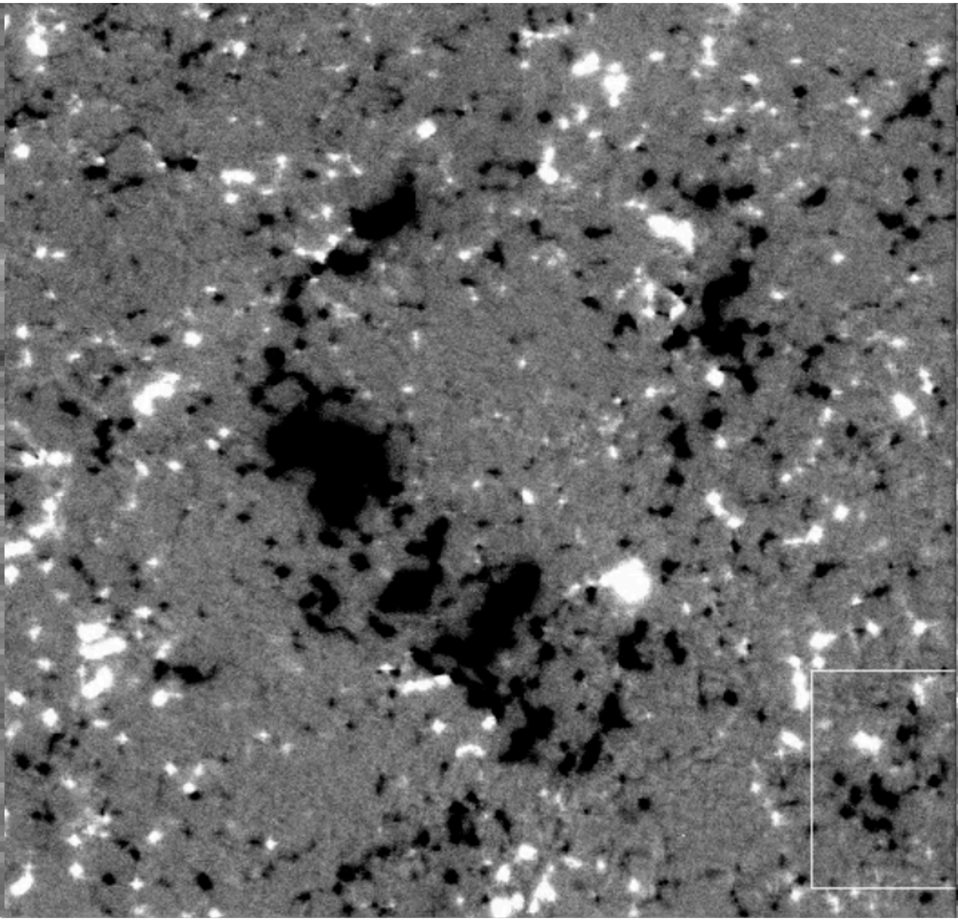

Hinode/NFI – longitudinal magnetogram HOP 151

HMI is blind to internetwork fields. Sensitive filtergraphs/spectrographs are a must

The importance of temporal resolution

Hinode/NFI, 02 Nov 2010, duration 39 hr, cadence 90s

Gošić et al., 2014, ApJ, 797, 49

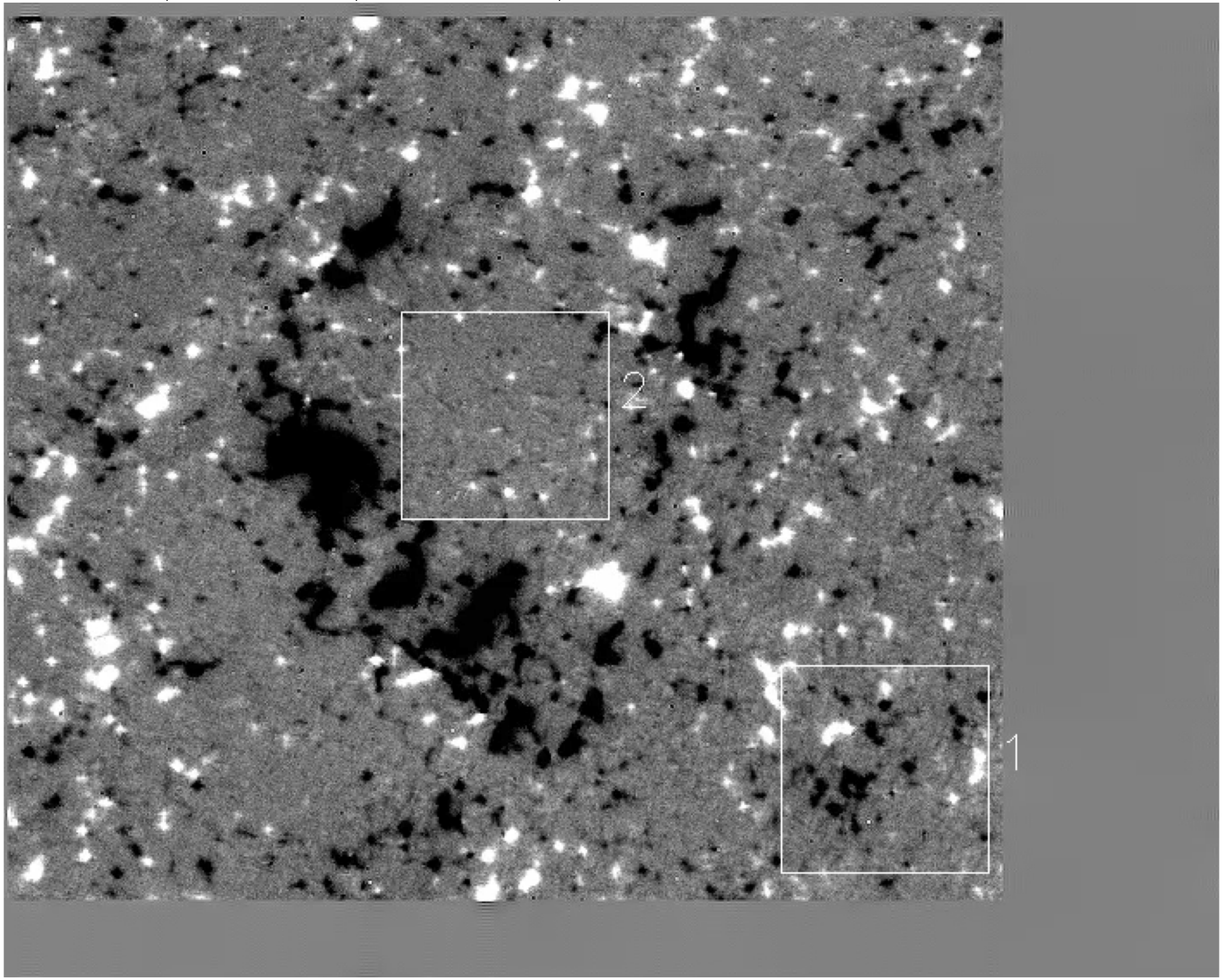

Quiet Sun fields emerge, interact with each other, and disappear from surface continually

Magnetic flux budget of the quiet Sun

Gošić et al., 2014, ApJ, 797, 49

Hinode/NFI Na D1 + automatic feature tracking

First determination of temporal evolution of internetwork flux

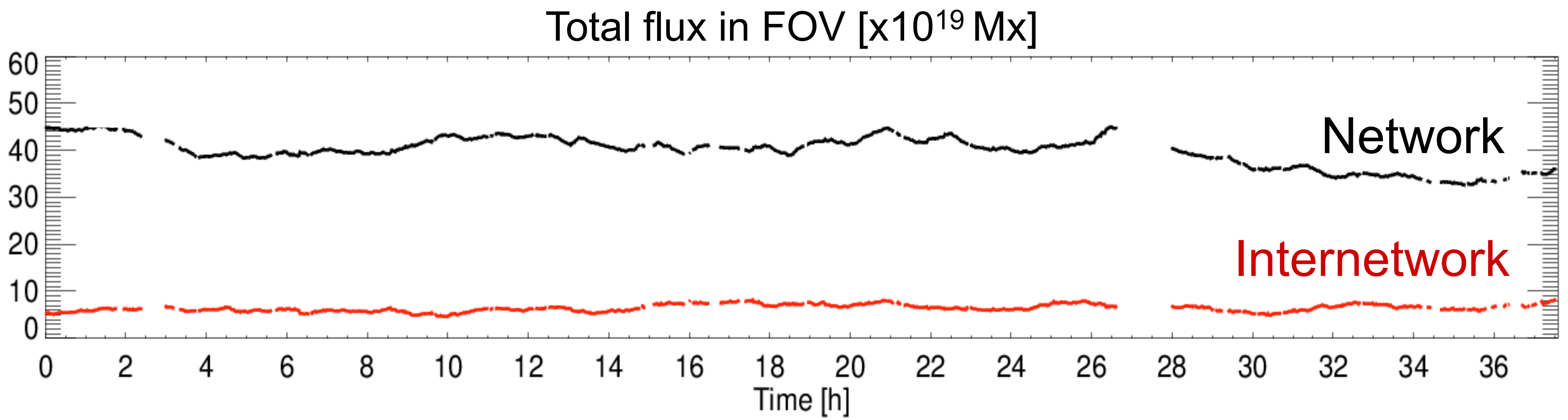

- NE flux over entire solar surface: ~ 7 x 10^{23} Mx
- IN flux over entire surface: ~ 1 x 10^{23} Mx
- AR flux at solar max: ~ 6 x 10^{23} Mx (Jin et al. 2011; solar cycle 23)

NE + IN fields carry more flux than ARs at solar maximum (and these are lower limits!)

Main open questions

- Magnetic field properties
- Magnetic flux and energy budget
- Evolution and interaction with ambient fields
  - Magnetic energy release
  - Effects in photosphere/chromosphere
- Maintenance of network/internetwork
- Origin of small-scale fields
  - small-scale vs global dynamo
  - Comparison with MHD simulations
  - Magnetic topology
  - Modes of appearance
  - Temporal evolution

The magnetic network

- Network outlines boundaries of supergranular cells (~30,000 km)
- Supergranules show diverging horizontal flows from center to edges and downflows at the boundaries
- Preferential site for accumulation of magnetic flux

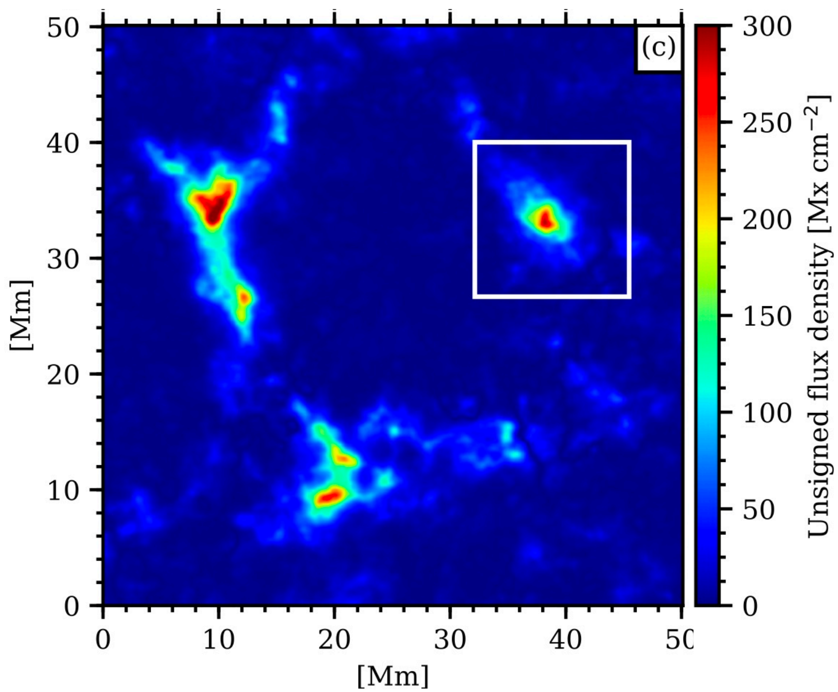

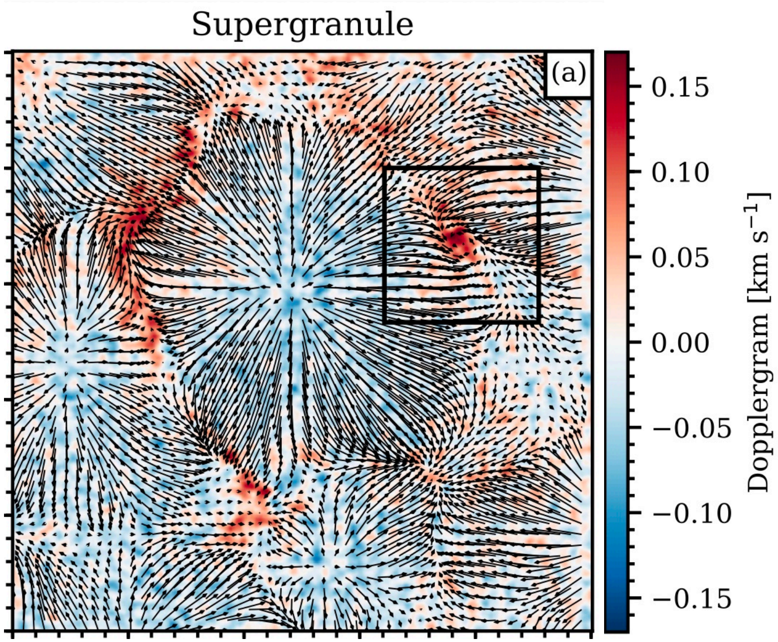

Requerey et al., 2018, A&A, 610, A84

The magnetic network

Strong network flux concentrations seem to be associated with persistent downflows and magnetic vortex flows at supergranular boundaries

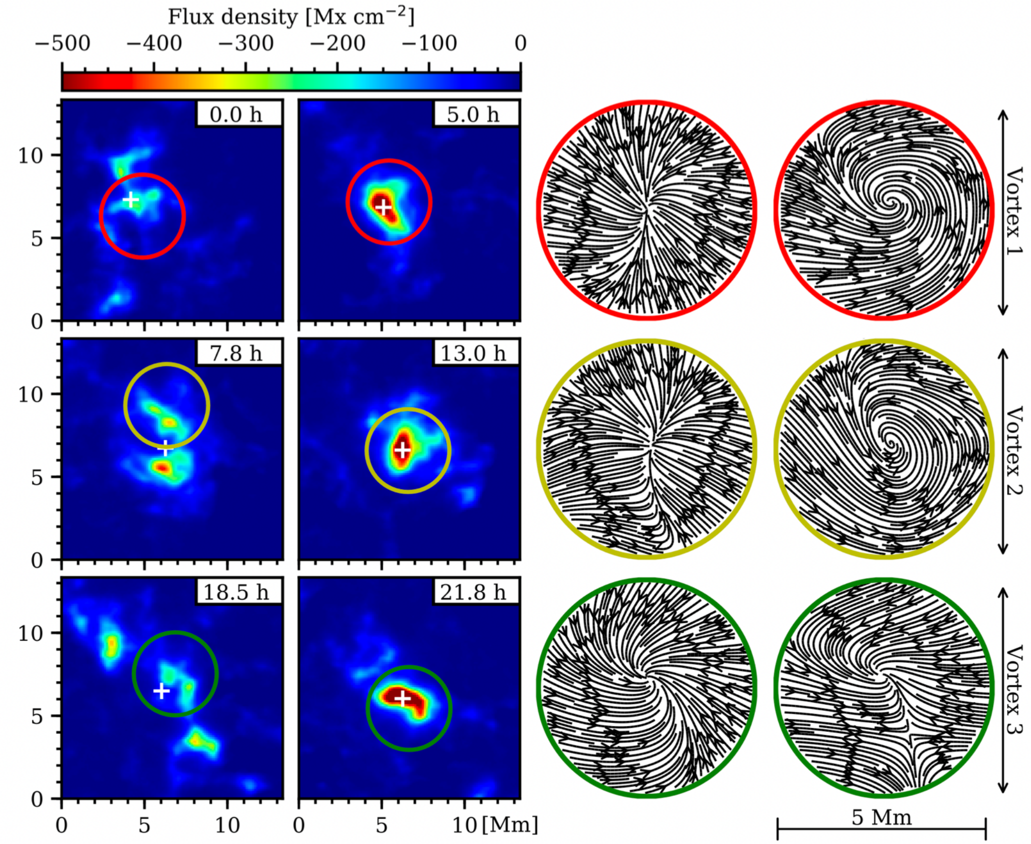

- Network element visible during 24 hours
- Three vortex flows observed over entire lifetime
- Element show stronger donwflows and field intensification during vortices
- Vortex stabilizes magnetic elements (Schüssler 1984)
- Vortex flows can explain network patchy appearance

Requerey et al., 2018, A&A, 610, A84

Network flux concentrations

- Network flux concentrations consists of vertical kG fields located in intergranular lanes
- Can be seen as bright points in continuum intensity/molecular bands
- Continuously interact with granular convection

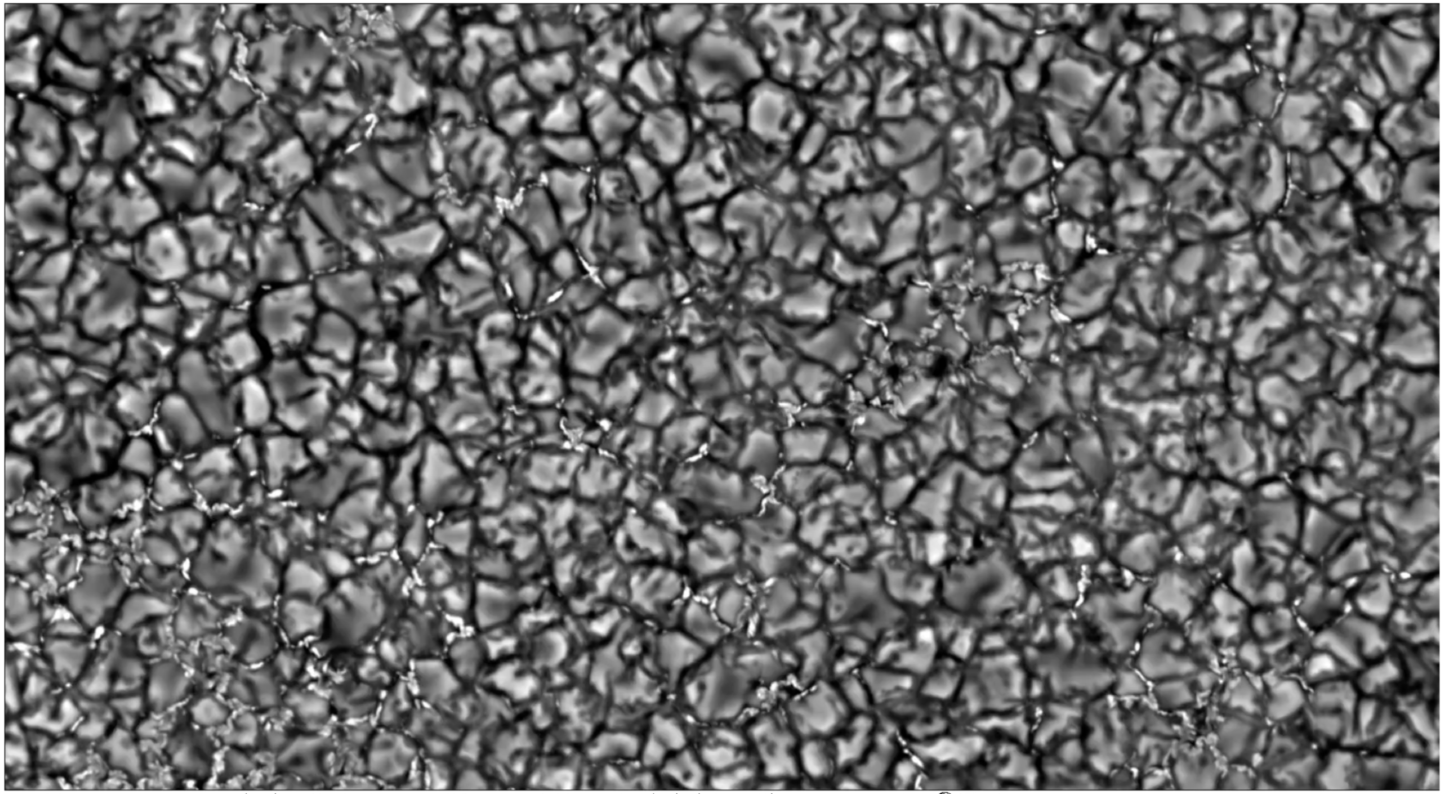

Swedish 1–m Solar Telescope (SST), CHROMIS Wideband 395.0 nm, 25–May–2017, (x,y)=(36",−91"), 01:08:02 duration 12742 km

Network flux concentrations

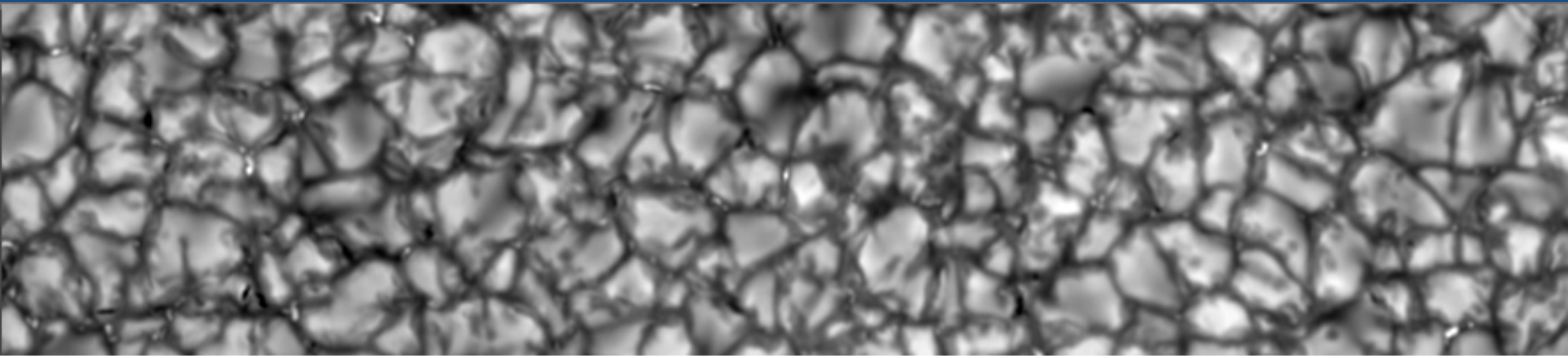

SST/CRISP, continuum intensity at 617 nm (0.15")

- Modeled as thin flux tubes (Spruit 1976)
- Magnetic field fans out with height, embedded in non-magnetic surroundings
- Diameters of 100-200 km at tau=1
- Formed by convective collapse (Parker 1978)

- Physical properties inferred from spectropolarimetric data at 1" resolution

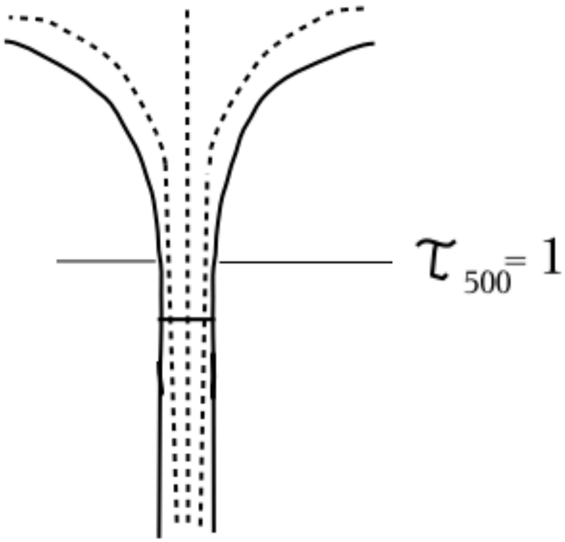

Howard & Stenflo (1972), Stenflo (1973), Stenflo et al. (1984), Solanki (1986), Solanki (1993), Keller et al. (1990), Keller (1992), Rüedi et al. (1992), Martínez Pillet et al. (1997), Bellot Rubio et al. (1997, 2000), Frutiger & Solanki (2001)

Structure of kG magnetic flux tubes

Inversion code based on thin flux tube model

- vertical tube
- 2 atmospheres
- hydrostatic equilibrium
- horizontal pressure balance
- flux conservation

Free parameters

- T_{mag} and T_{ext} with height
- v_{mag} and v_{ext} with height
- $B(z_0)$, $P_{ext}(z_0)$, $r(z_0)$
- v_{mac}, v_{mic}, stray light

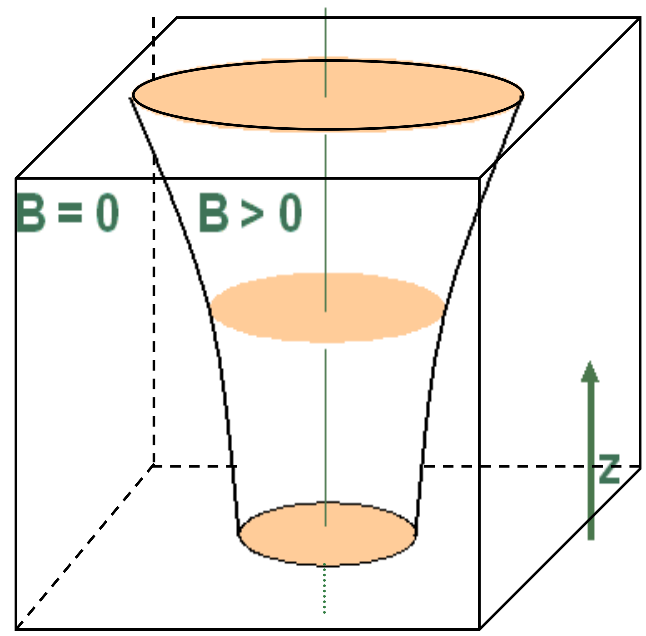

Applied to Stokes I and V profiles with 1” spatial resolution

Structure of kG magnetic flux tubes

Bellot Rubio et al., 2000, ApJ 535, 489

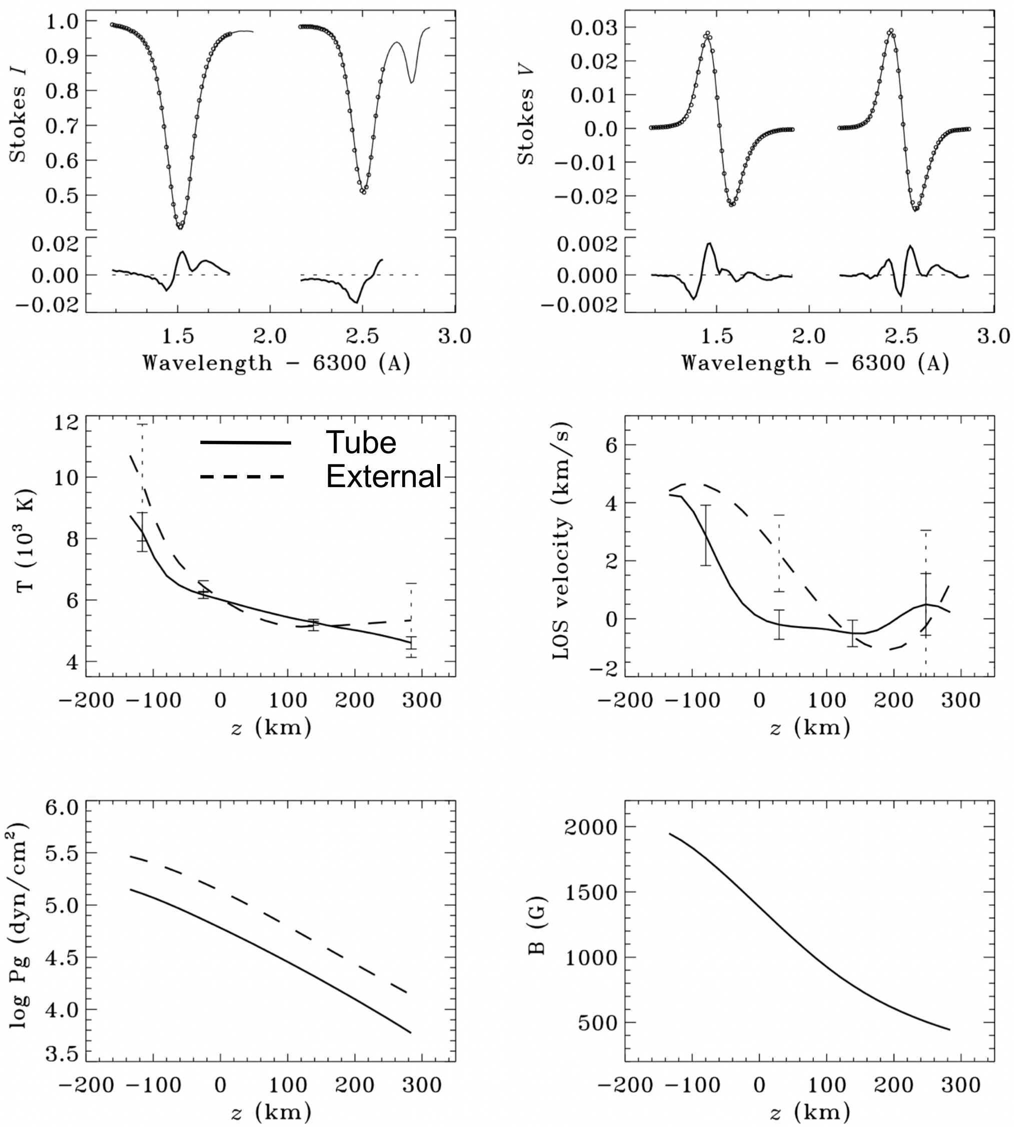

- B = 1380 G at z=0 km
- r = 110 km at z=0 km

- Tube is cooler than external surroundings in deep photosphere
- Tube is hotter than external surroundings higher up

- Strong internal downflows of up to 4 km/s below z=0 km
- Strong external downflows

Semi-empirical model explain Stokes V asymmetries and confirms theoretical predictions

Structure of kG magnetic flux tubes

Bellot Rubio et al., 2000, ApJ 535, 489

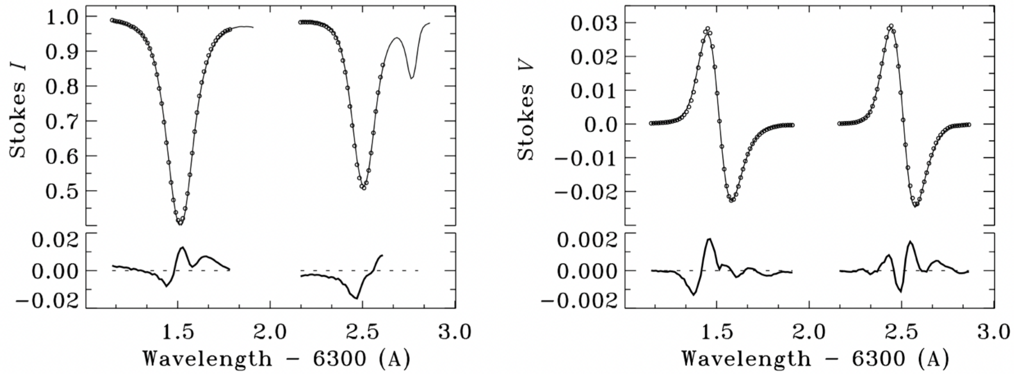

$$\delta A \equiv \frac{|A_\mathrm{b}| - |A_\mathrm{r}|}{|A_\mathrm{b}| + |A_\mathrm{r}|} = 2.8\%$$

$$\delta a \equiv \frac{|a_\mathrm{b}| - |a_\mathrm{r}|}{|a_\mathrm{b}| + |a_\mathrm{r}|} = 10.9\%$$

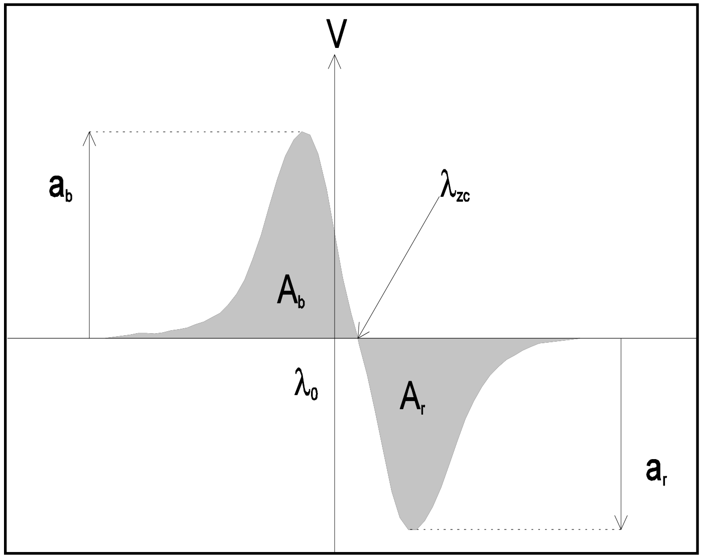

Structure of kG magnetic flux tubes

Bellot Rubio et al., 2000, ApJ 535, 489

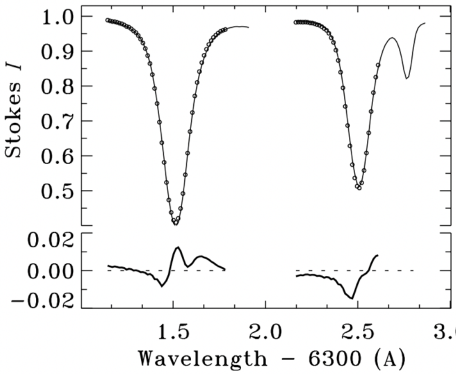

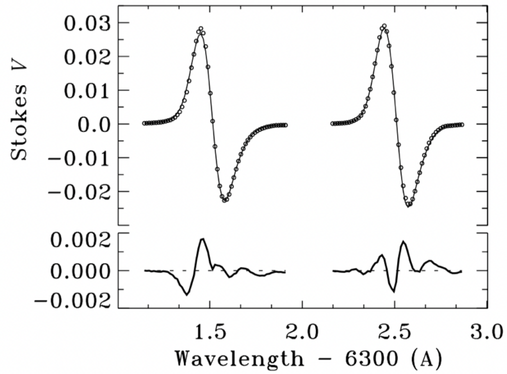

$$\delta A \equiv \frac{|A_{\rm b}| - |A_{\rm r}|}{|A_{\rm b}| + |A_{\rm r}|} = 2.8\%$$

$$\delta a \equiv \frac{|a_{\rm b}| - |a_{\rm r}|}{|a_{\rm b}| + |a_{\rm r}|} = 10.9\%$$

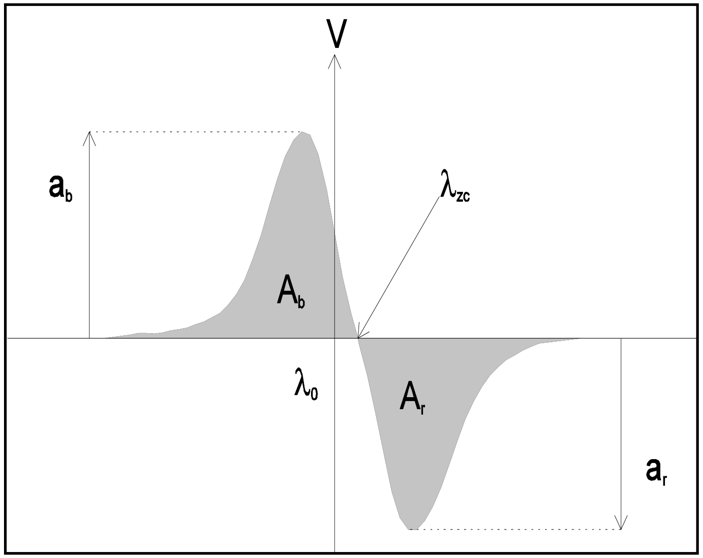

The area asymmetry is due to gradients of atmospheric parameters along LOS (Auer & Heasley 1978)

$$\mathrm{sign}(\delta A) = -\mathrm{sign}\left(\frac{\mathrm{d}v_{\rm LOS}}{\mathrm{d}\tau} \cdot \frac{\mathrm{d}B}{\mathrm{d}\tau}\right)$$

$$\mathrm{sign}(\delta A) = -\mathrm{sign}\left(\frac{\mathrm{d}v_{\rm LOS}}{\mathrm{d}\tau} \cdot \frac{\mathrm{d}|\cos\gamma|}{\mathrm{d}\tau}\right)$$

Solanki & Montavon (1993)

Structure of kG magnetic flux tubes

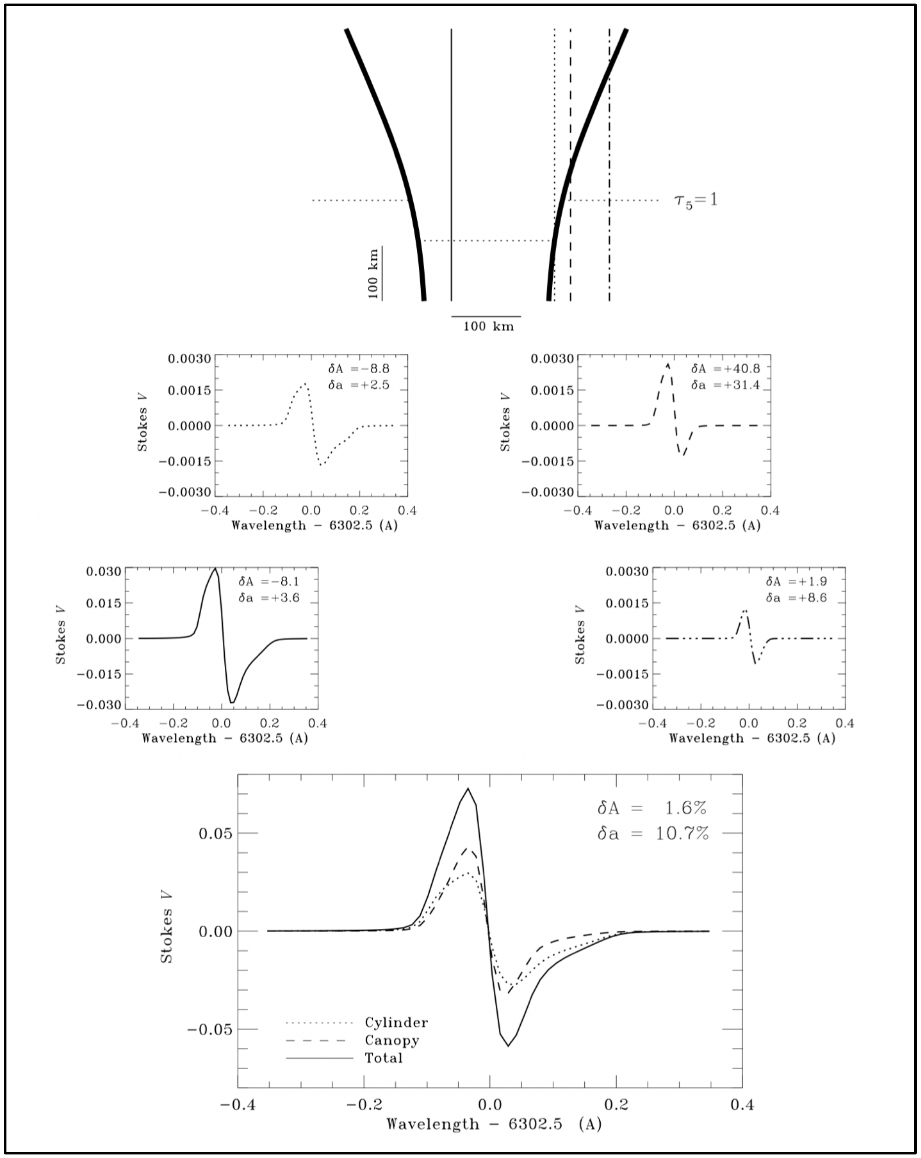

- Canopy produces positive area and amplitude asymmetry
- Central core produces negative area asymmetry and positive amplitude asymmetry
- Sum of all rays produces small positive area asymmetry and large amplitude asymmetry, in accordance with observations

Structure of kG magnetic flux tubes

3D MHD simulations

Flux tubes are cooler than their surroundings at equal geometric height, but their radiation emerges from deeper, hotter layers, producing bright points

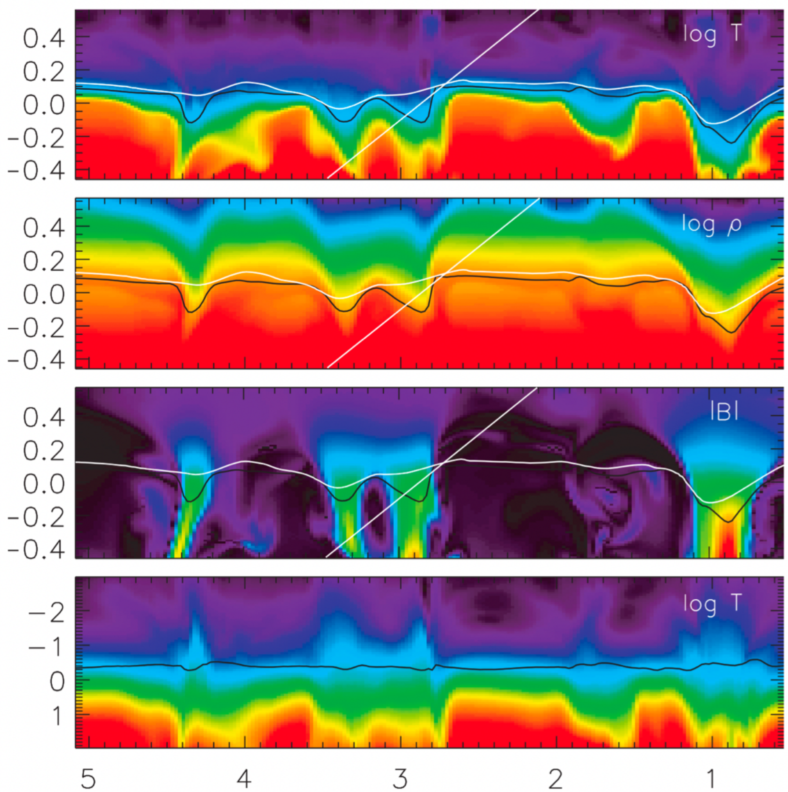

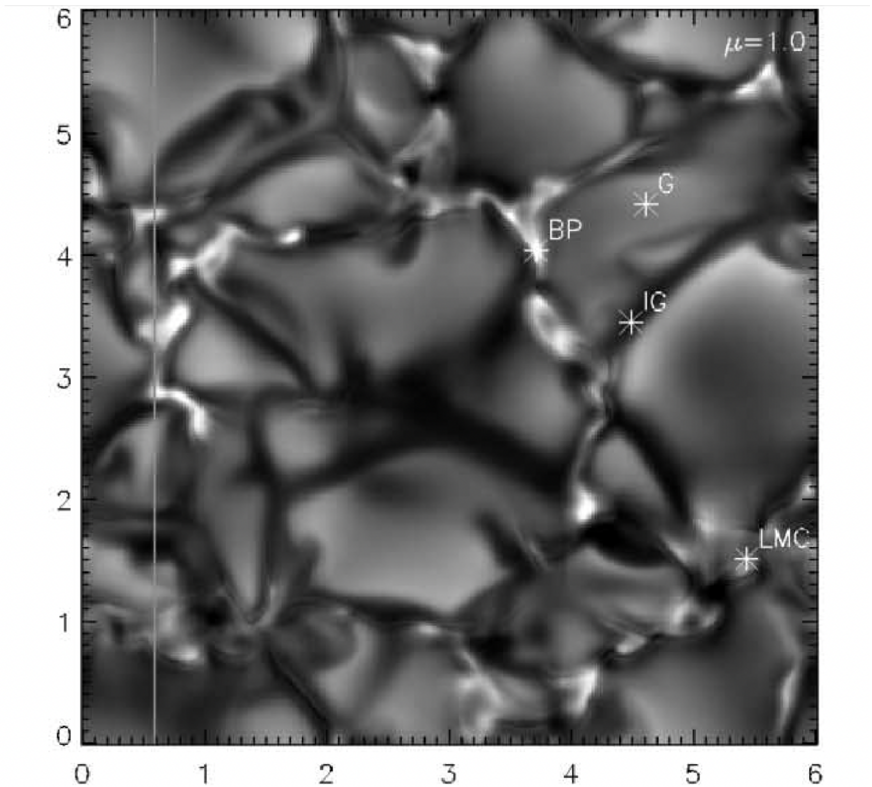

Carlsson et al., 2004, ApJ 610, L137

Structure of kG magnetic flux tubes

2D MHD simulations

External downflow jets occur at the boundaries of the flux tube, due to the cooling of the gas resulting from the lateral heat influx into the tube

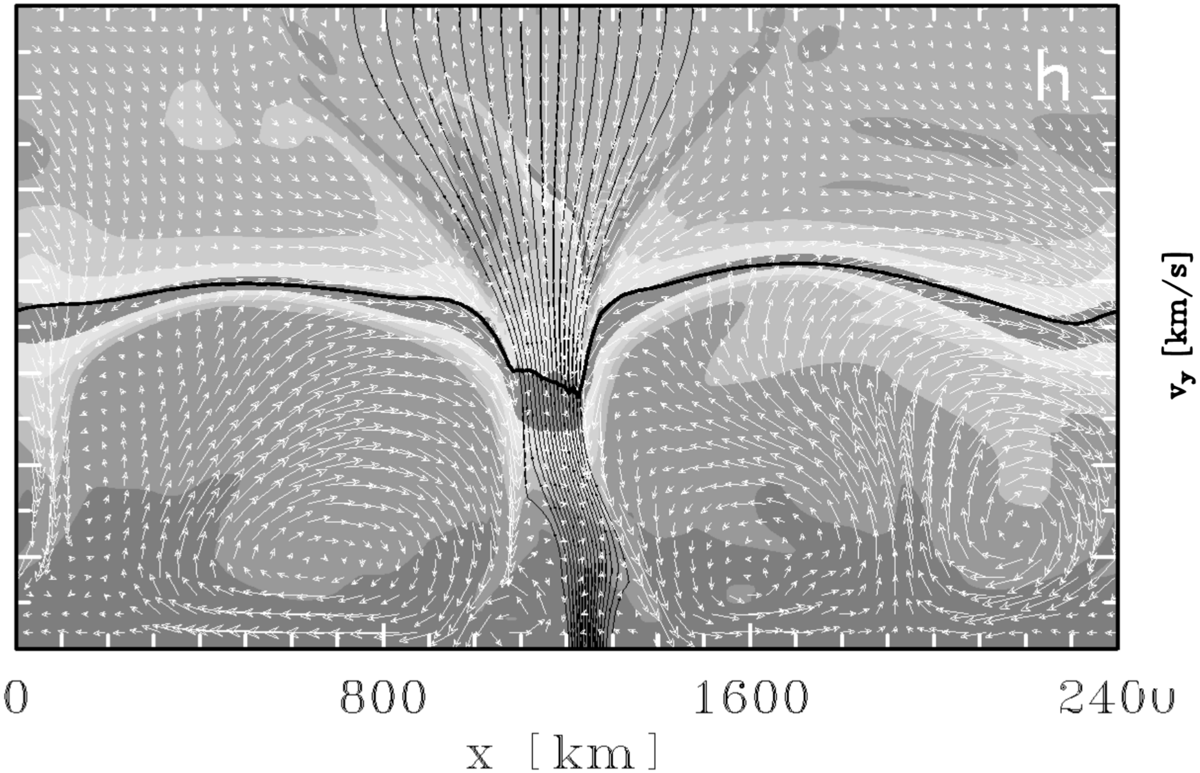

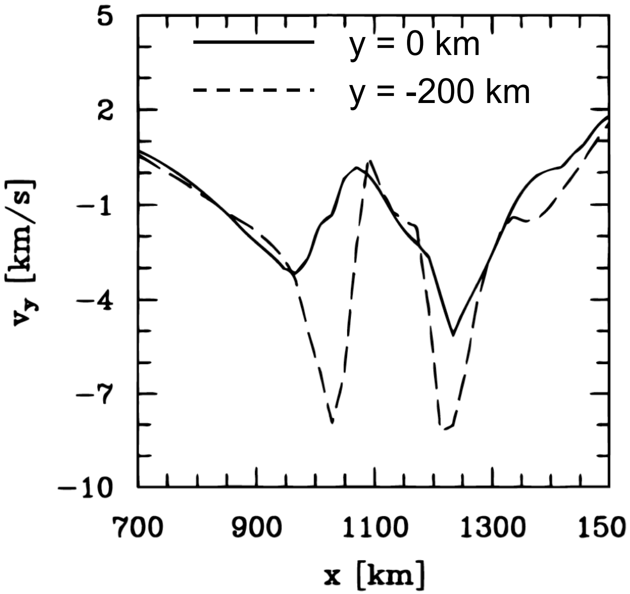

Steiner et al., 1998, ApJ 495, 468

Structure of kG magnetic flux tubes

Langangen et al, 2007, ApJ, 655, 615
SST/TRIPPLE Fe I 5380 + simulations

Velocity field in and around QS magnetic ribbons/flowers

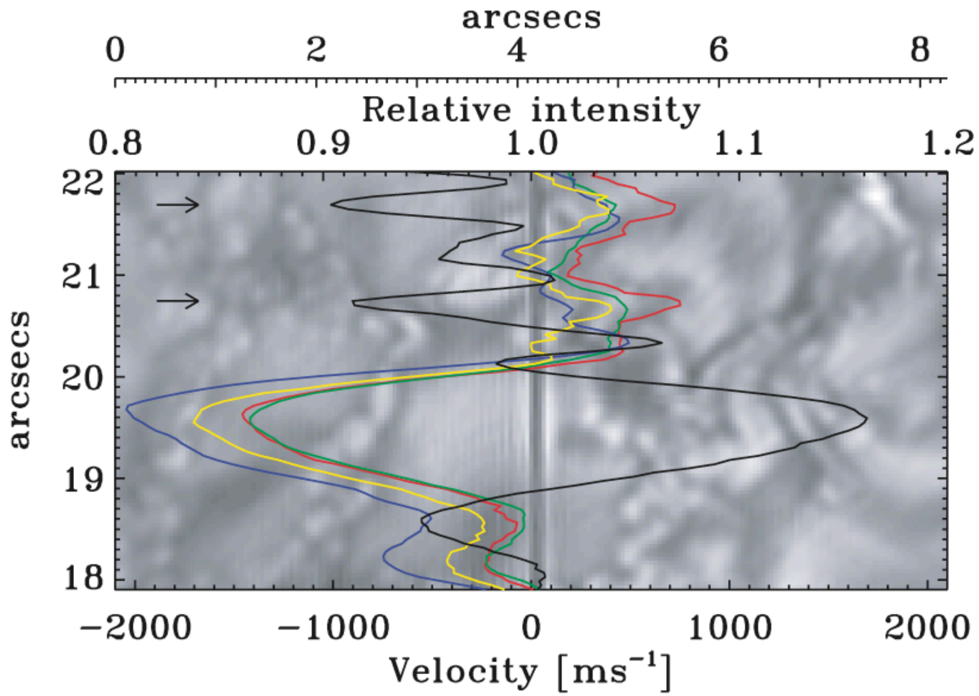

Velocity at intensity level of 0.85
Velocity at intensity level of 0.65
Continuum intensity at 5380

- Narrow sheets of downflows adjacent to magnetic ribbons and flowers
- Downflows increase with depth, up to ~0.8 km/s near continuum forming layers
- Small downflows inside the magnetic structures
- Comparison with 3D simulations suggests flows are actually larger

First direct visualization of the external downflows inferred from Stokes inversions at 1"-resolution (Bellot Rubio et al. 1997)

Structure of kG magnetic flux tubes

Buehler et al., 2015, A&A, 576, A27

Hinode/SP normal map + 2D spatially coupled inversion

3D magnetic and dynamic structure of plage flux tubes

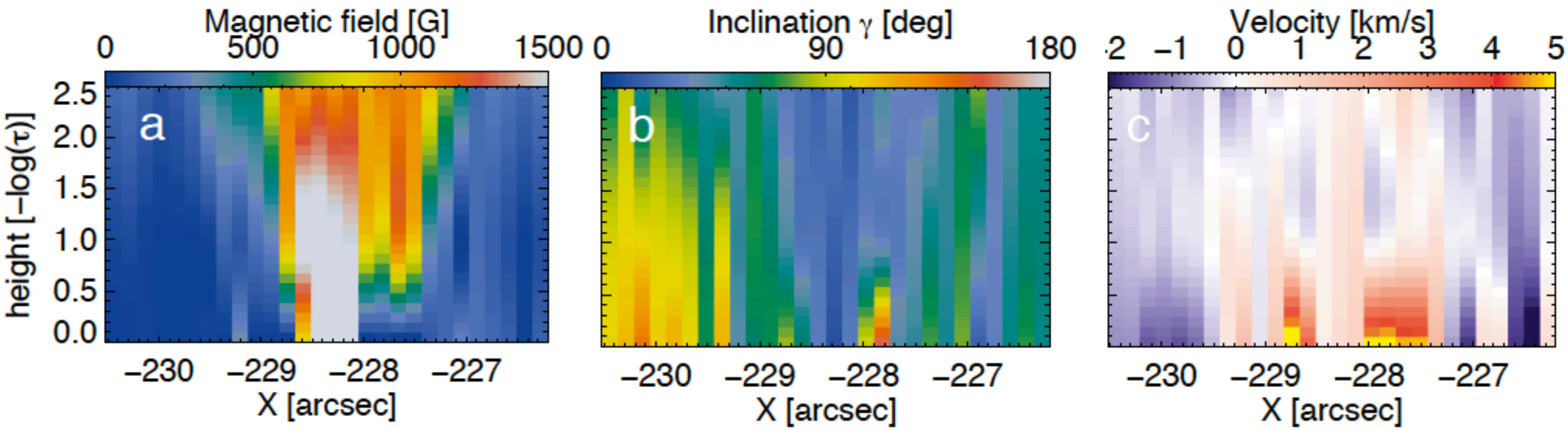

- Resolved flux tubes expanding with height
- Mean field strength of 1520 G at log tau=-0.9
- Ring of strong downflows surrounding the flux concentration in deep layers, up to 10 km/s (previously detected through Stokes inversions by Bellot Rubio et al. 1997)
- Weak (<300 G) patches of opposite polarity ouside the flux concentration in deep layers (also reported by Scharmer et al. 2013)

Structure of kG magnetic flux tubes

Scharmer et al., 2013, A&A, 553, A63

SST/CRISP + stray-light compensation + NICOLE inversion

3D magnetic and dynamic structure of network flux tubes

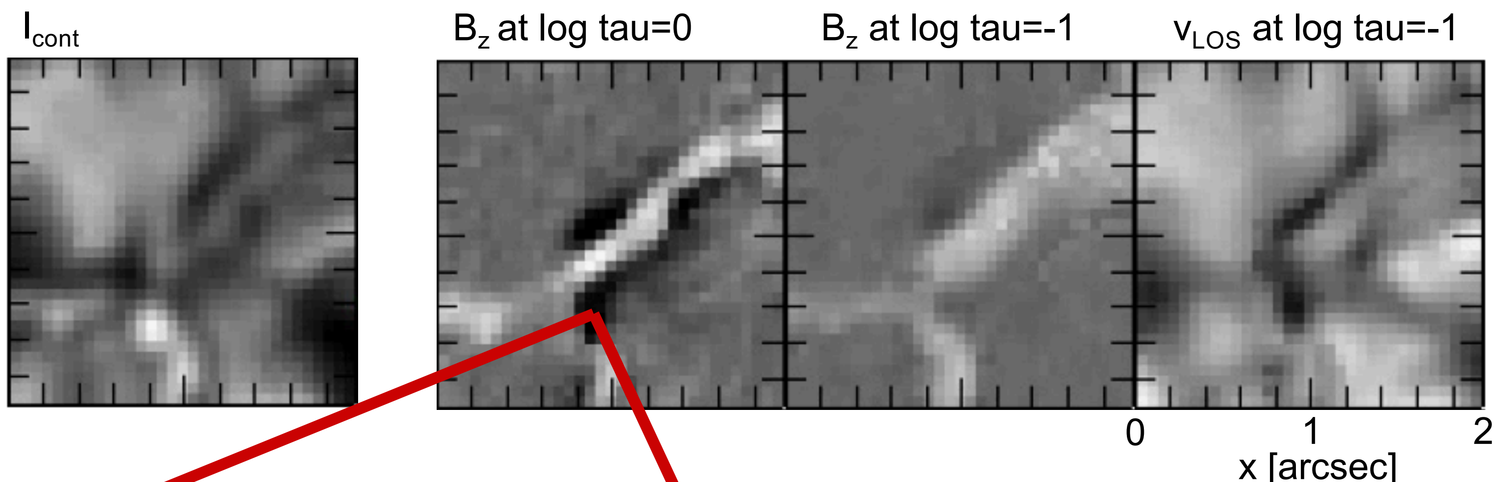

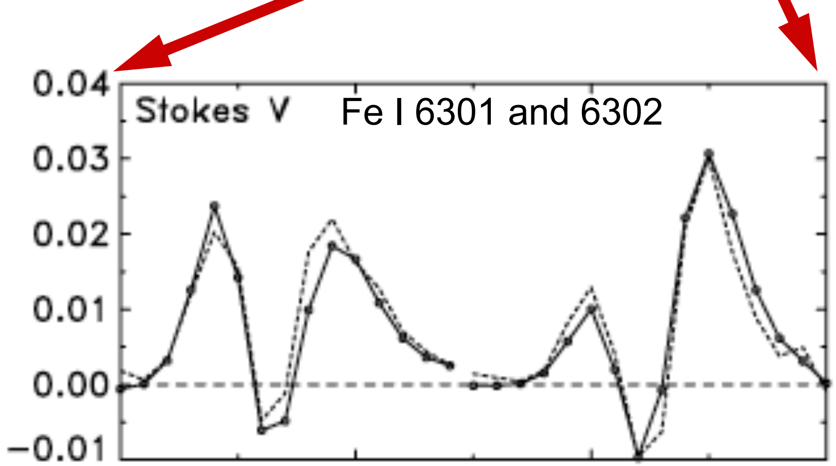

Tiny narrow sheets of *strong*, opposite polarity field at the boundaries of some network flux concentrations

Structure of kG magnetic flux tubes

Lagg et al, 2010, ApJ, 723, L164

SUNRISE/IMaX Fe I 5250.2 + phase diversity + SPINOR inversion

Fully resolved network magnetic flux tubes

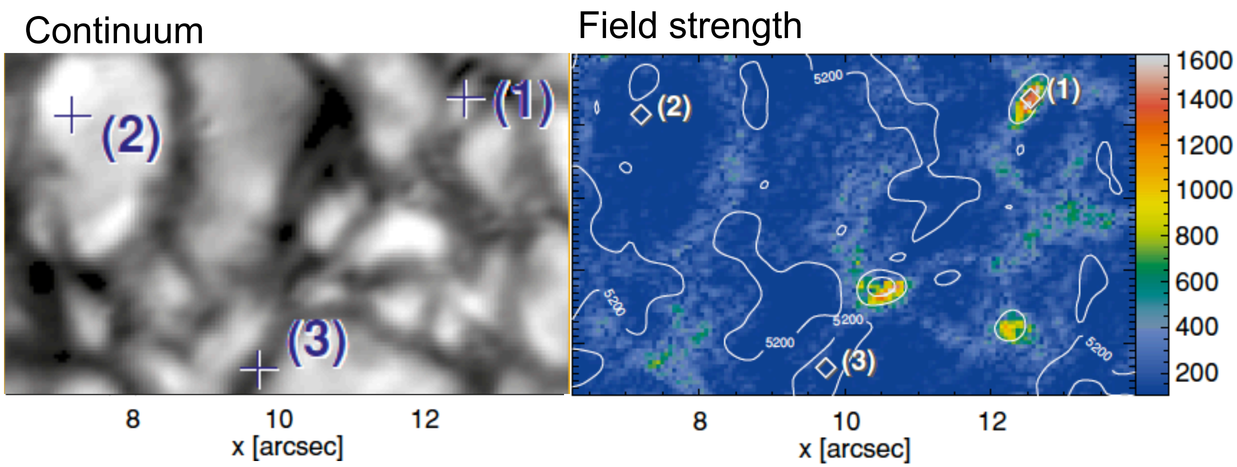

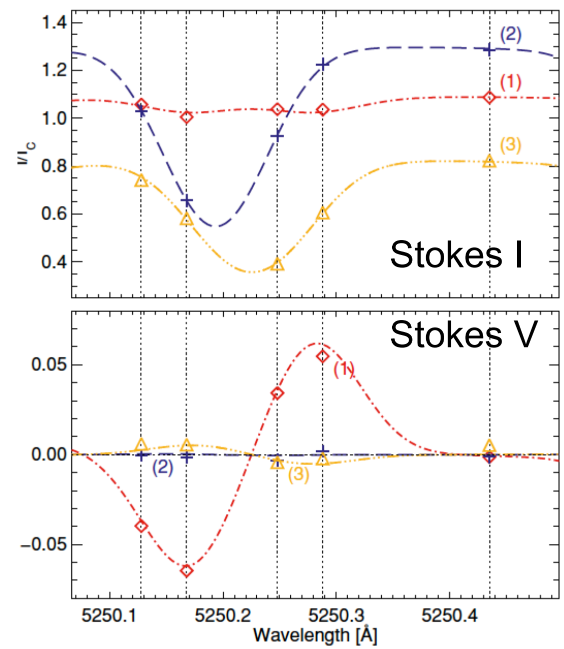

- Very weak Fe I 5250.2 nm Stokes I profile from network patch
- Profiles well fitted in terms of a one-component model atmosphere
- Field strength of 1450 G
- Strong temperature enhancement of ~1000 K at log tau=-2
- Consistent with semiempirical plage flux tube models

First time Stokes profiles are explained with a magnetic filling factor unity

Structure of kG magnetic flux tubes

Martínez González et al., 2012, ApJ, 758, L40

SUNRISE/IMaX L12-2 + SIRJUMP inversion

Magnetic canopy of network flux concentrations characterized

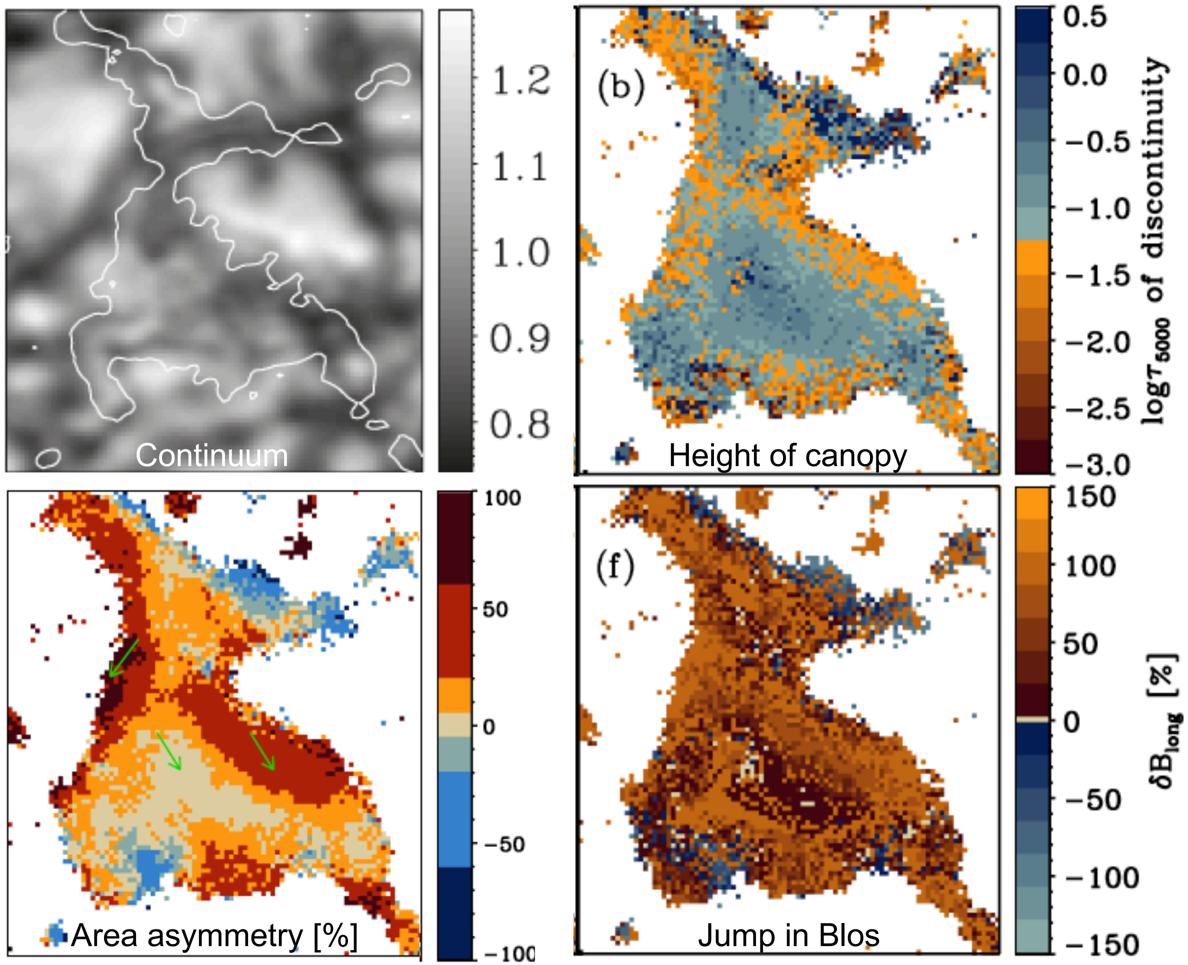

- Clear pattern of Stokes V area asymmetries
- Discontinuity of parameters along the LOS signals the presence of canopy
- Height of canopy increases with radial distance from patch center
- Relative jump of B_{long} increases toward edges

Formation of kG flux concentrations

- Problem: how to amplify the field up to kG values?
- Several-step process
- Flux expulsion (Parker 1963)
  - Magnetic fields, being frozen in the photospheric plasma, are swept into the intergranular lanes by horizontal convective flows
  - This kinematic effect concentrates field up to equipartition values (~500 G)
- Superadiabatic effect (Parker 1978)
  - The magnetic field inhibits convective heat transport, and the gas becomes an excellent thermal insulator. Adiabatic motion.
  - A gas parcel moving downwards in the tube becomes cooler and denser than the surroundings, and continues to move downwards
  - The gas is not replenished through the tube's walls
  - As a result, the tube's interior is evacuated
  - To maintain horizontal pressure balance, the field is intensified

Convective collapse

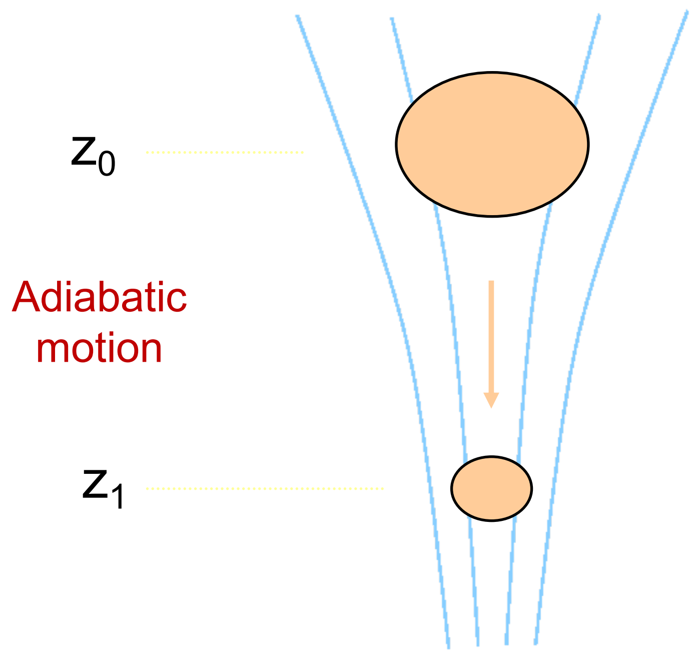

$T_{int} = T_{ext}$
$P_{int} = P_{ext}$

$T_{int} < T_{ext}$
$P_{int} = P_{ext}$ $\Rightarrow$ $\rho_{int} > \rho_{ext}$

Strong donwflows evacuate the tube, so internal gas pressure decreases

The tube is compressed from the outside, its cross section is reduced and the field strength increases because of flux conservation

Convective collapse

The superadiabatic effect requires an initial donwflow. Spruit & Zweibel (1978) found that tubes having less than 1300 G are convectively unstable

The instability sets in either as a *downflow* or as an *upflow*

DOWNFLOWS — Amplification of the field by the superadiabatic effect

UPFLOWS — The reverse process takes place and a decrease in the field strength ensues

Spruit (1979) showed that downflows lead to final states with field strengths of 1-2 kG. He called this process convective collapse

The spectropolarimetric signatures of convective collapse are large redshifts and increasing Stokes V signals

Formation of kG flux concentrations

Bellot Rubio et al., 2001, ApJ, 560, L1010

VTT/TIP + SIR inversions

Convective collapse and upward moving fronts

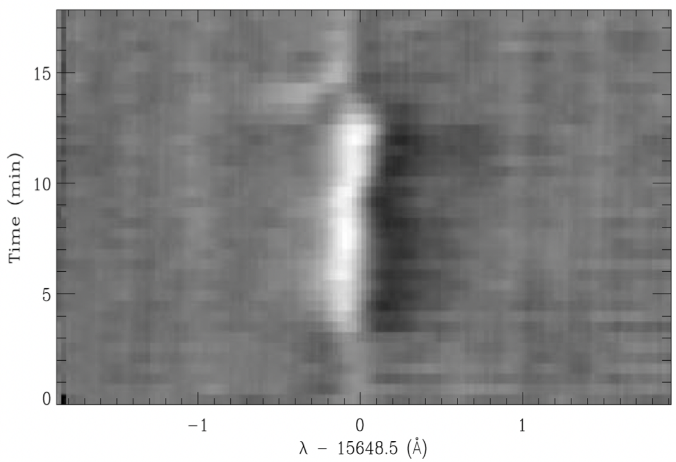

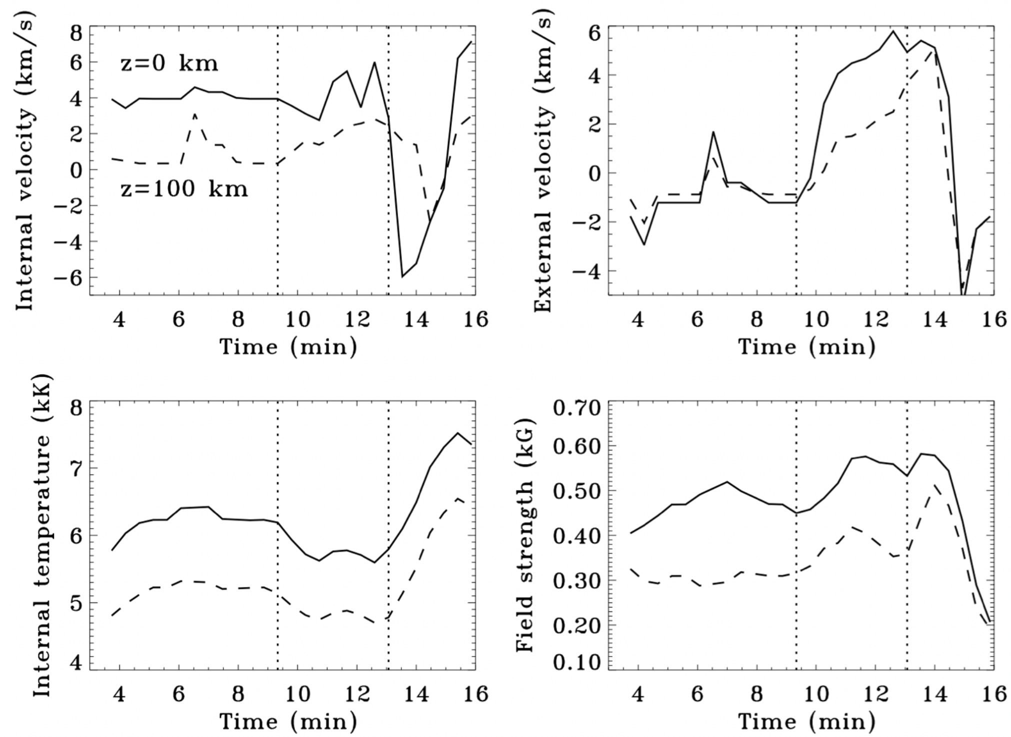

- **Flux expulsion (~10 min)** Moderate redshifts and downflows, B increases very slowly
- **Convective collapse (~3 min)** Large redshifts, strong downflows, B increases from 400 to 600 G
- **Upward moving front (~2 min)** Large blueshits, strong upflows, B decreases from 600 to 200 G

Formation of kG flux concentrations

Nagata et al., 2008, ApJ, 677, L145

Hinode/SP dynamic mode + ME inversions

Convective collapse

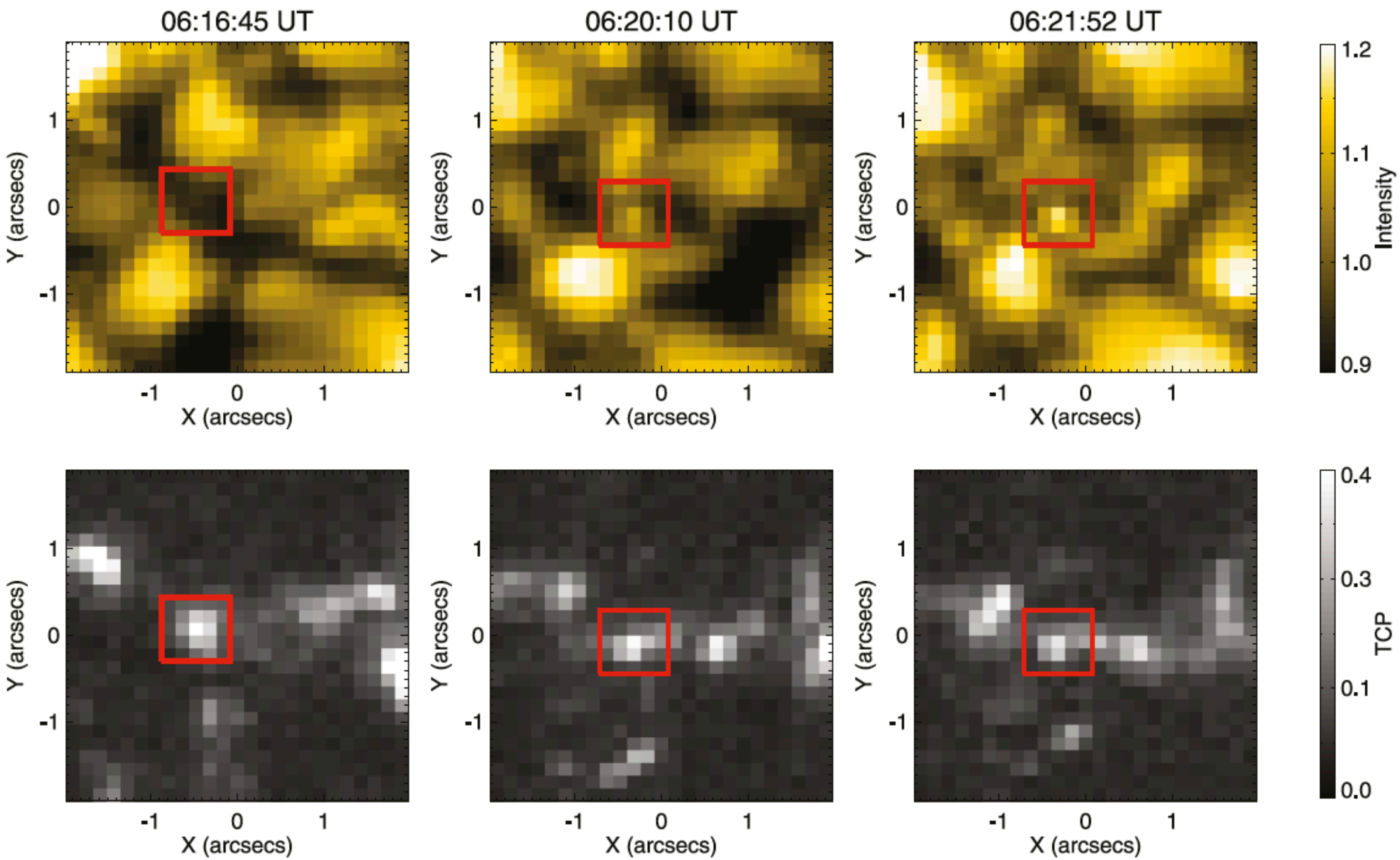

Formation of kG flux concentrations

Nagata et al., 2008, ApJ, 677, L145

Hinode/SP dynamic mode + ME inversions

Convective collapse

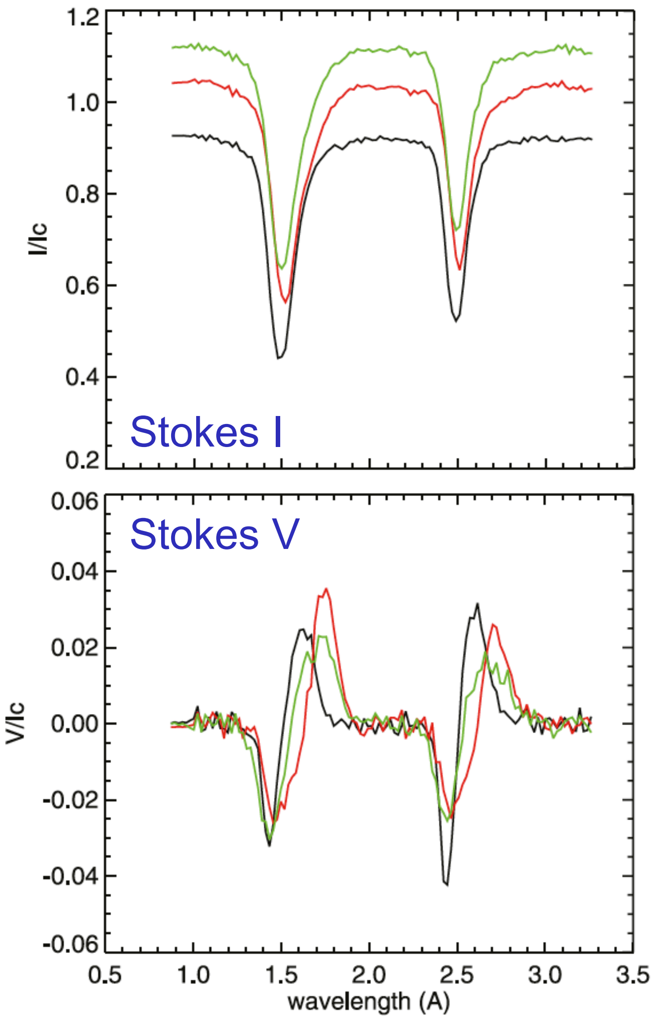

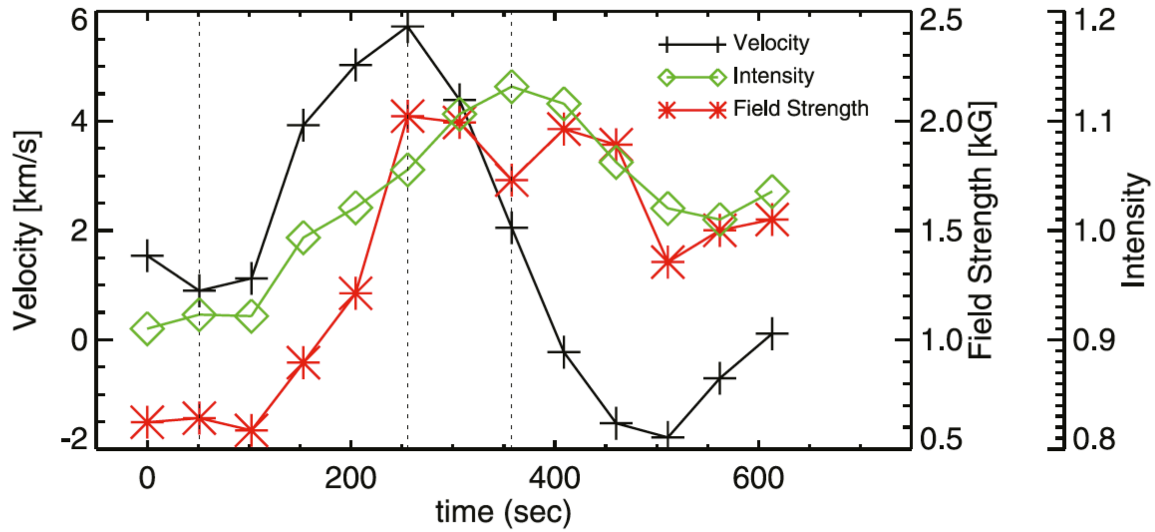

- Strong downflows of up to 6 km/s
- Field increases from equipartition values up to 2 kG
- Formation of bright point in continuum intensity after magnetic field reaches its maximum
- End result is stable strong magnetic feature (1.5 kG)
- Compatible with convective collapse (Parker 1978)

Formation of kG flux concentrations

Fischer et al., 2009, A&A, 504, 583

Hinode/SP + NFI Mg I b_2 Dopplergrams + Ca II H filtergrams + ME inversions

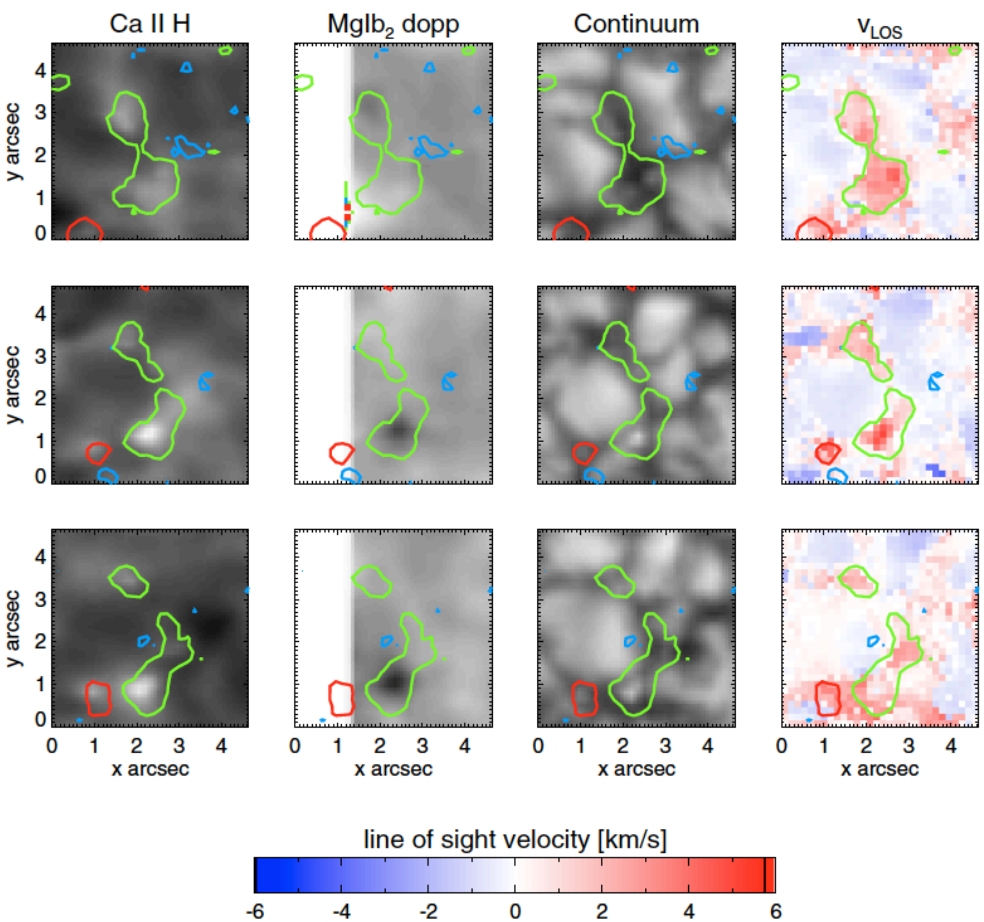

Convective collapse

- Statistical study of 49 events
- Strong photospheric downflows
- Field intensification up to 1.7 kG
- Brightenings in continuum intensity
- Nearly all cases associated with brightenings in Ca II H filtergrams
- Mean duration ~10 min

About three quarters of the events also show downflows in upper photosphere

No stable kG features formed!

Formation of kG flux concentrations

Narayan, 2011, A&A, 504, 583

SST/CRISP Fe I 6302 + ME inversions

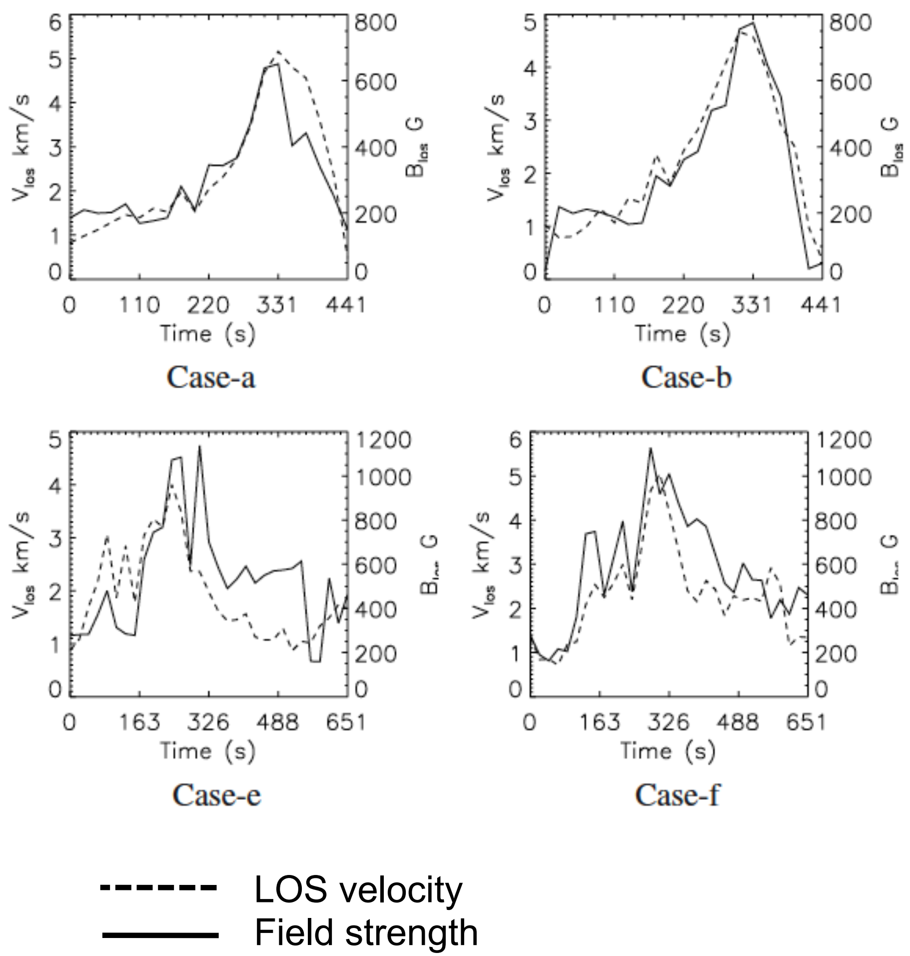

Convective collapse

- Eight events observed
- Short duration (<10 min)
- Field intensification up to 1.2 kG in response to strong downflows of up to 5 km/s
- Brightenings in continuum intensity

No stable kG features formed: magnetic field decreases back to equipartition values soon

Formation of kG flux concentrations

Requerey et al, 2014, ApJ, 789, 6
SUNRISE/IMaX V5-6 + SIR inversions

First complete description of the formation and evolution of individual features in QS

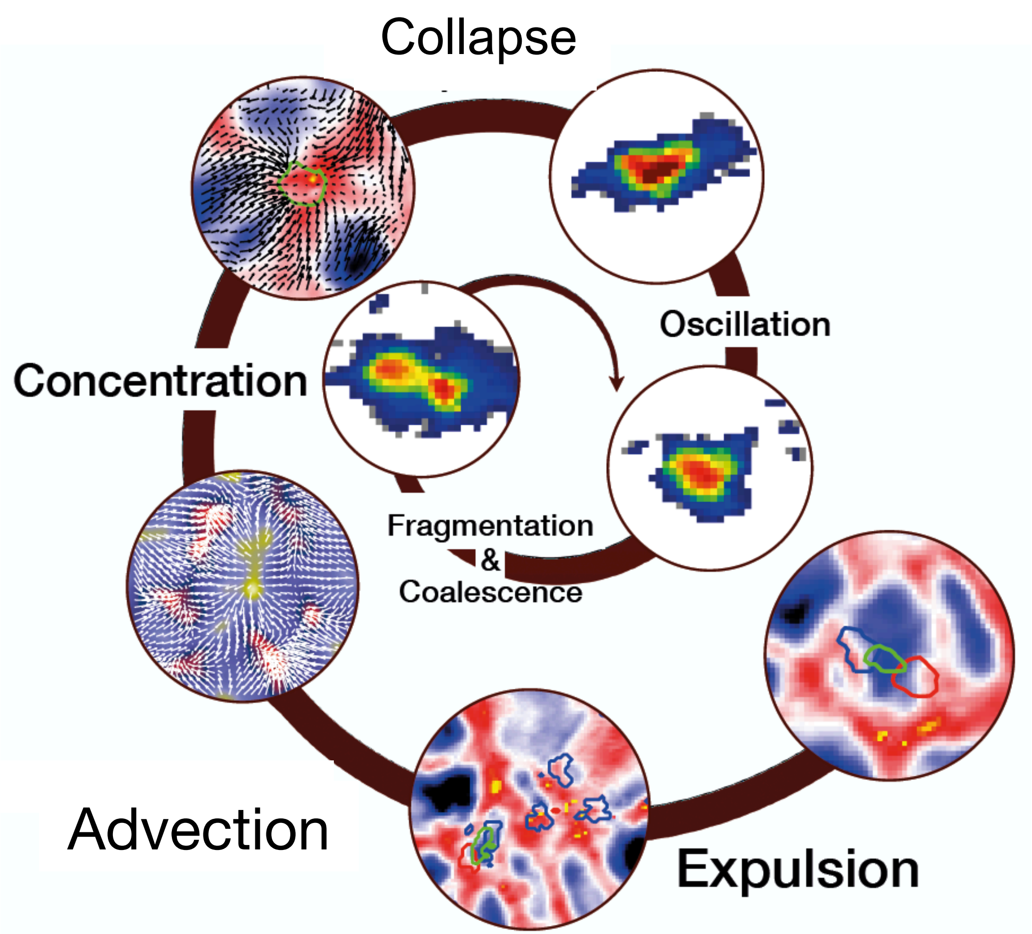

The lifetime of QS elements

- Formed by flux expulsion and concentration of flux by granular/mesogranular advection
- kG field strengths reached through convective collapse
- BPs and upflow plumes
- Mature elements show oscillations in field strength, velocity and area (Martínez González et al. 2011)
- Interaction with external flows is the driver of many of the changes

Magnetic elements undergo processes going beyond the simple physics of flux tubes

Origin of the magnetic network

- **Enhanced network:** decay of active regions
- **Quiet network:** ephemeral regions
  - 90% of the network flux comes from ERs (Martin 1990)
  - Network flux can be replaced by ERs in 1.5–3 days (Schrijver et al. 1997)
  - Network flux can be replaced by ERs in 8-19 h (Hagenaar et al. 2003)
  - Paradigm based mainly on MDI observations

Ephemeral regions

- “Small” magnetic bipoles
- Emerge near the center of supergranular cells
- Early papers
  - Dodson (1953), citing Babcock
  - Harvey & Martin (1973)
  - Harvey et al. (1975)

- Pole separation: ≤ 20"
- Horizontal speed: ~ 4 km/s
- Flux: 1-300 x 10^{18} Mx
- Mean flux: ~ 10^{19} Mx
- Lifetime: ~ 4 h

BBSO magnetogram, ± 50 Mx cm^{-2}

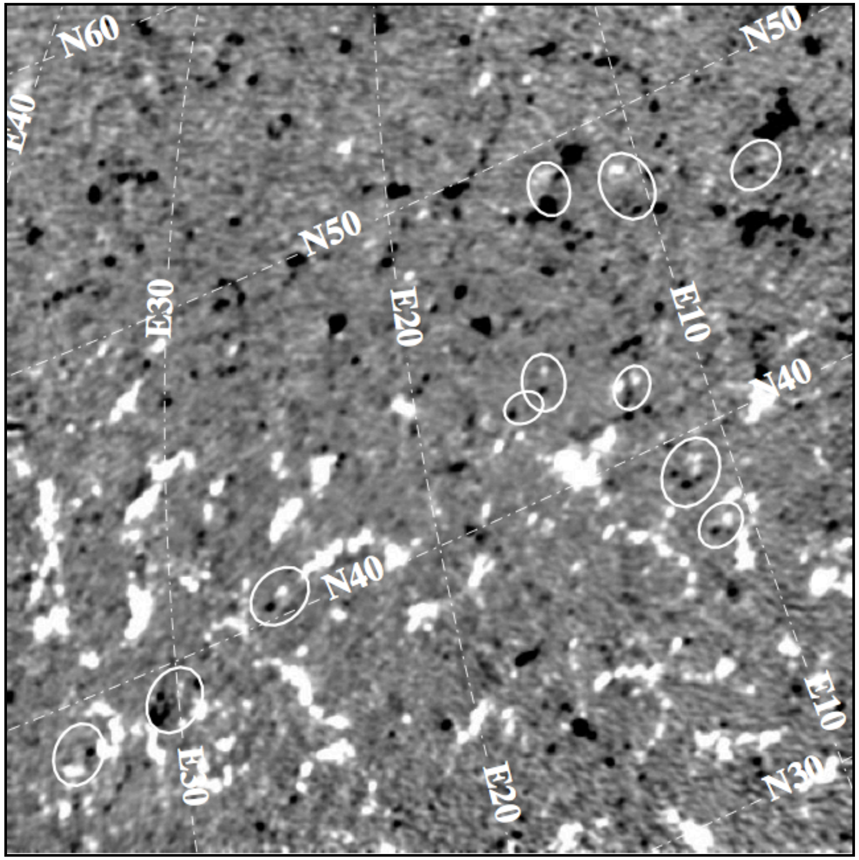

Chae et al. (2001)

Ephemeral regions

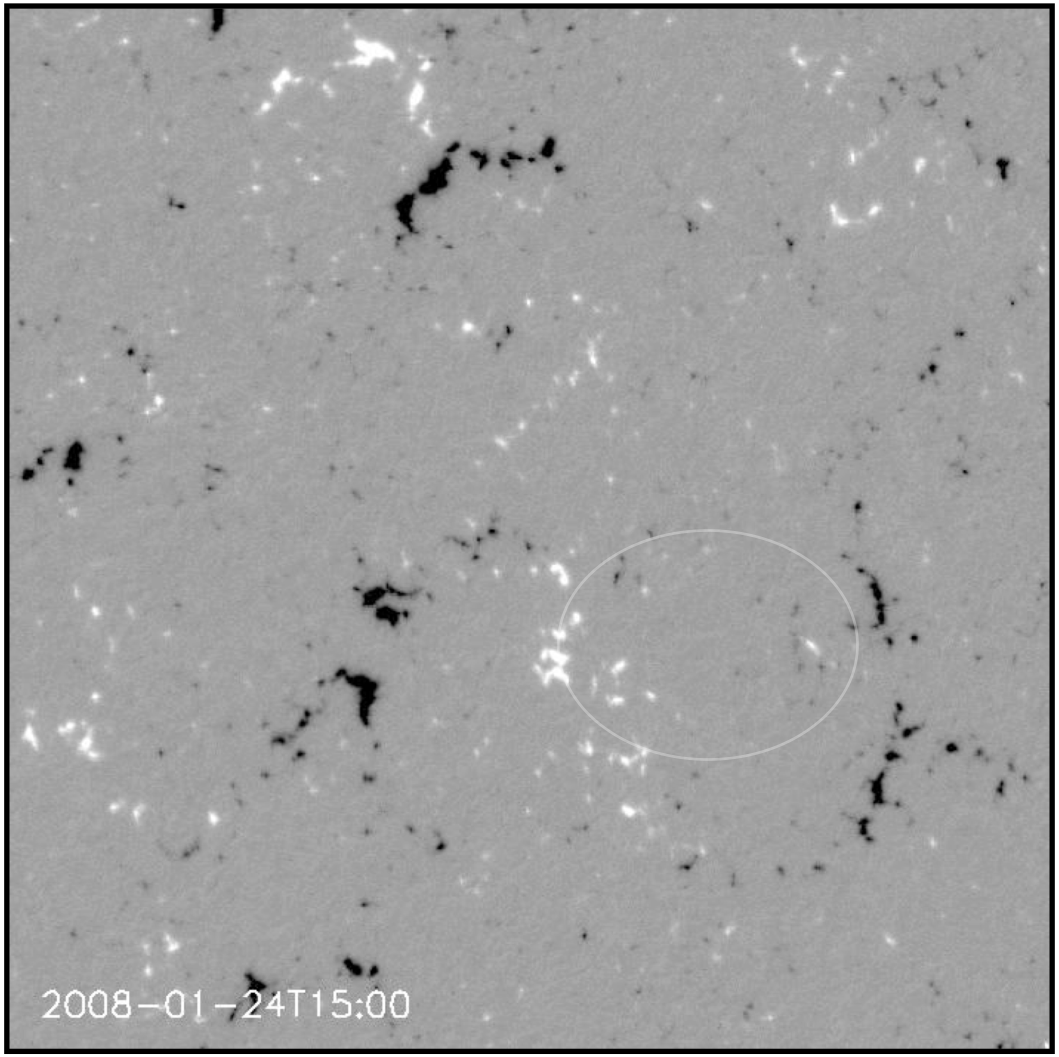

Hinode/NFI
Na I 589.6 nm
Cadence: 3 min
FOV: 112" x 112"

At high spatial resolution, ephemeral regions are detected as clusters of small-scale, mixed-polarity features

Network
Merging
Cancellation

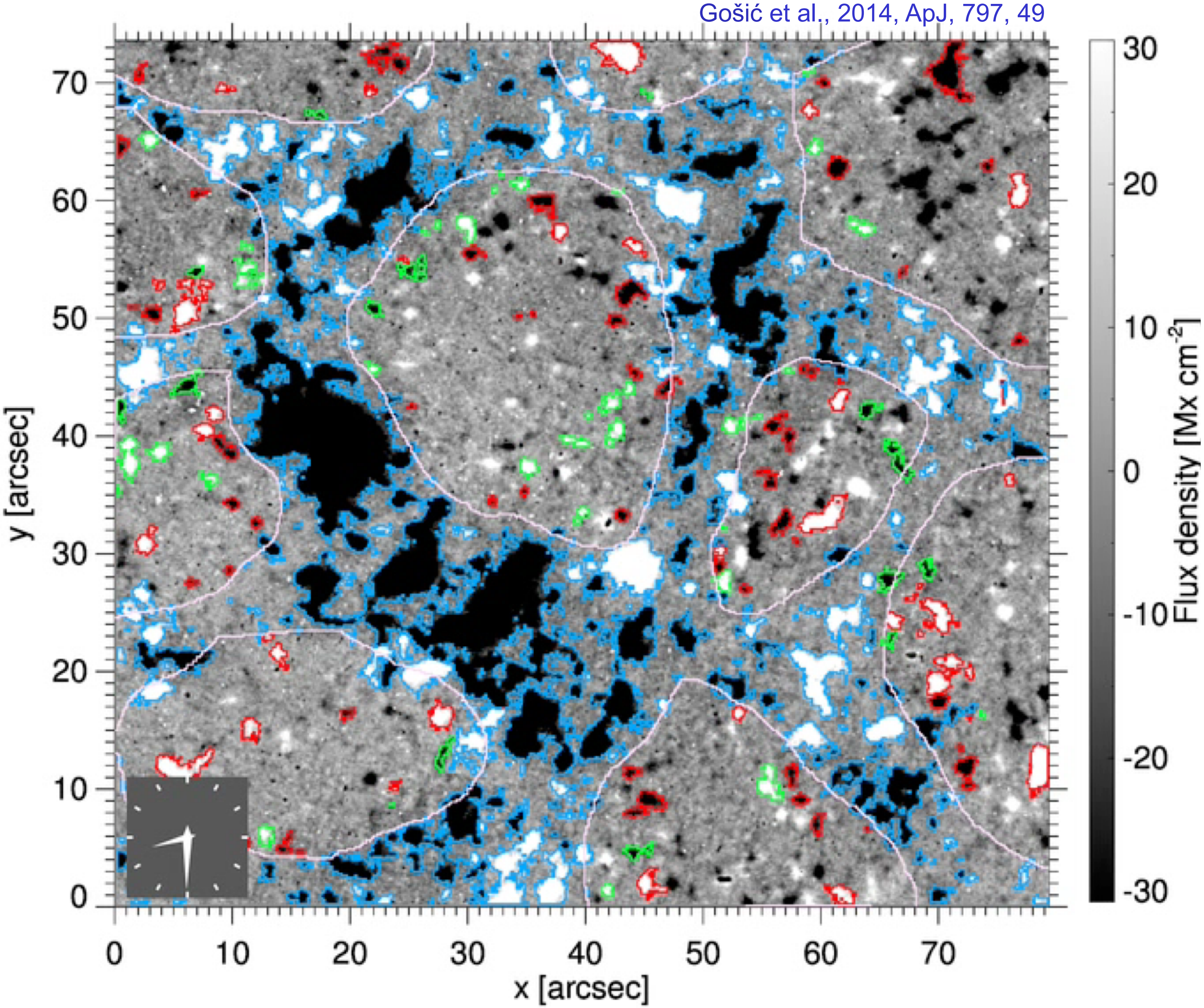

Eventually, 38% of total IN flux gets transferred to the network

IN flux transfer to the network

Gošić et al., 2014, ApJ, 797, 49

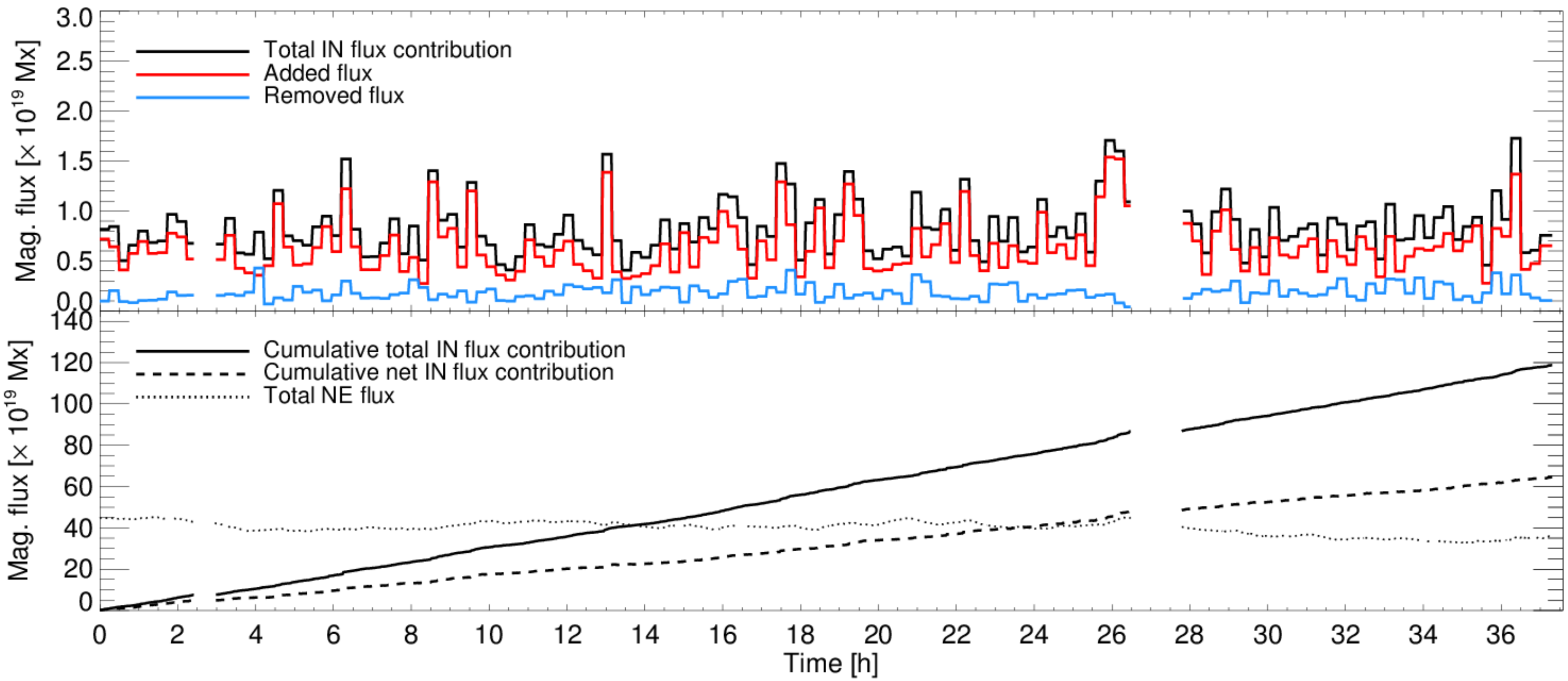

IN contributes 1.6 x 10^{24} Mx day^{-1} to the network over entire solar surface

IN capable of replenishing network flux in only ~14 h

But the network flux does not increase indefinitely…

There must be a way to get rid of the flux supplied by the IN!

IN flux transfer to the network

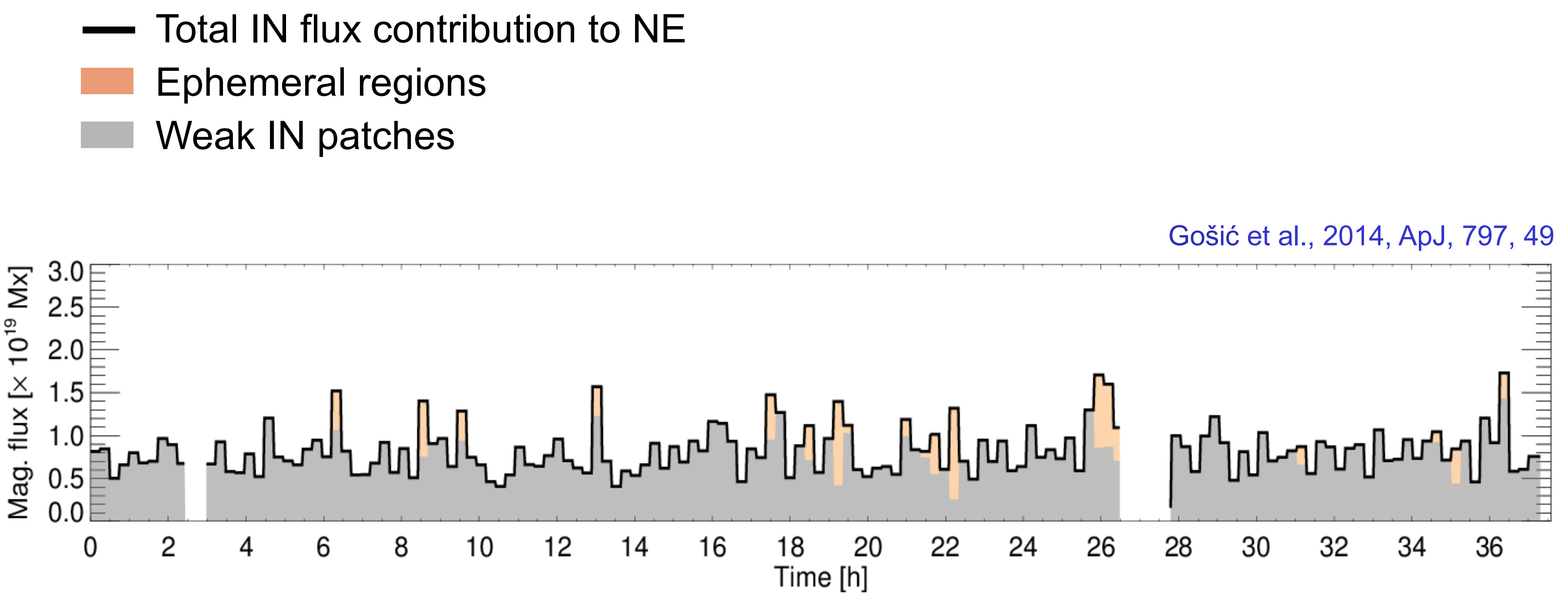

CHANGE OF PARADIGM

The IN is the main source of flux for the network

(Ephemeral regions account for only 10% of total IN contribution to NE)

But the network flux does not increase indefinitely

There must be a way to get rid of the flux supplied by the IN